Behavior of Soil Salinity Sensors

By

RAMON LUIS ARAGUES
Grad. (University of Zaragoza, Spain) 1973

THESIS

Submitted in partial satisfaction of the requirements for the degree of

MASTER OF SCIENCE

in

Water Science

in the

GRADUATE DIVISION

of the

UNIVERSITY OF CALIFORNIA

DAVIS

Approved:

Committee in Charge

Deposited in the University Library .....
Date *Librarian*

This work is dedicated to the memory of my father, whose silent presence has guided my effort.

ACKNOWLEDGEMENTS

I would like to express my thanks and appreciation to Dr. J. W. Biggar and Dr. D. W. Henderson whose guidance and direction were most valuable in all aspects of the investigation and thesis preparation. The suggestions of Dr. D. Rolston were most helpful in the final review of this work. Thanks are due to Dr. L. D. Whittig who assisted me with the X-ray analysis of the samples and its interpretation, and to my friend J. F. Juste for his help with the computer program.

I would like to acknowledge the friendship and assistance of Otavio De Camargo, whose support and discussions aided greatly to the completion of the work. Dr. R. J. Wagenet is thanked for his friendship and support when I first came to the department. Jim MacIntyre and Bob Jackson helped me in the laboratory and Mr. Charlie Brown and Mr. Renold Nelson in the modification and construction of some of the apparatus I used in the experimental work.

Financial support from Instituto Nacional de Investigaciones Agrarias. Spain, is acknowledged.

Finally, my wife and son shown an unbelievable amount of love and patience during the last two years of my graduate study. Their understanding made this work more meaningful to me.

TABLE OF CONTENTS

INTRODUCTION

One of the greatest single problems facing much of the world population today is the production of food and fiber. This implies the necessity of both increasing land productivity of present agricultural areas as well as the development of new areas for agricultural purposes. In many instances both objectives will have to face ecological problems.

At present salt problems are seriously reducing the value and productivity of millions of hectares all over the world. For illustration purposes, the total area of the earth's land surface is approximately 75 billion hectares, and about one-third of this has been classified as arid and semi-arid. Only 3% of these arid and semiarid areas are irrigated at present, although the potentially irrigable land may exceed 4 billion hectares. A greater proportion of the irrigable lands would have been under production by now if it were not for the uncertainties resulting from the development of salt-affected soils in the older irrigated areas. In fact, it is recognized that saline and alkali soil conditions were among the principal factors involved in the decline of many ancient civilizations.

From these considerations the need to maintain an ecological balance of present productive lands as well as the development of potentially new agricultural areas is well understood.

The best way to either control or reduce the salt concentration in the soil profile is to displace the solution from the root zone with water of lower salt concentration. The manner in which this leaching process proceeds - as well as does the salinization process - is an

important consideration. Therefore it is necessary to monitor the actual soil-water salinity with measuring devices. This is currently done by measuring the electrical conductivity (EC) of the soil solution which is proportional to the total amount of soluble salts present in the soil water.

The EC of the saturation extract has been used for years for appraising soil salinity, especially in relation to plant growth. Advantages of the method are that the saturation percentage water content is related to the field moisture range over a considerable textural range and therefore the soluble-salt concentration in the soil water in the field can be approximated from the saturation extract if the water content is known. Also, the extract can be analyzed for particular ions. Disadvantages of the method are: (i) soil samples must be taken, brought into the laboratory and the soil solution extracted before solutions can be analyzed. The time and work involved in this procedure is an important limitation if we want to measure the soil solution conductivity continuously as is the case in many management programs. (ii) The change in ion concentrations relative to each other between the soluble and exchangeable phases, and (iii) the inaccuracy of extrapolating salinity at saturation soil moisture to lower soil water contents, since the concentrations of dissolved salts in the soil solution do not usually change in direct proportion to changes in soil water contents. However, despite these limitations, the saturation extract continues to be one of the most useful methods for appraising soil salinity, especially in relation to plant growth.

The extraction of the soil solution <u>in-situ</u> using suction probes is useful only in a narrow range of high matric potentials (up to -0.6

bars), and therefore is impractical in many field situations. However, the method also permits the analysis of particular ions.

The determination of soil salinity with soil resistance measurements is an adaptation of earth resistivity techniques used by geophysicists, and involves the measurement of resistance between an array of electrodes that are placed in the immediate soil surface and over the location of concern. The four probe method eliminates many of the disadvantages mentioned above, but introduces the problem of correcting the changes in conductivity for varying water contents of the soil.

An alternative method for in-situ measurement of EC of the soil solution is the salinity sensor, which has become commercially available in the last few years. In some instances, a disadvantage of the salinity sensor is that rather than measuring bulk soil salinity, it responds to a small localized region within the soil body, and therefore numerous buried in-situ devices are needed to assess the salinity distribution within the soil profile. However, the simplicity and rapidity of the procedure for making measurements makes it a practical tool for monitoring soil salinity.

The salinity sensor uses the principle that spaced electrodes embedded in porous ceramic measures the EC of the salt solution in the ceramic. The method is based on the assumption that the concentration of salts within the porous insulator is in equilibrium with the ionic concentration of the adjacent soil-water solution, and that the porous ceramic remains saturated with soil water at all times. Thus, as long as the geometry of the water in the ceramic remains constant, the path of flow of electric current between the two electrodes, fired into the ceramic, is fairly constant and the unit is comparable to a regular

conductivity cell. Therefore we can use the relation

$$R \times EC = K$$

where R is the resistance of the cell and K is the cell constant. Since K for a given ceramic cell can be found by saturating it with a solution of a known conductivity and measuring R, the resistance of the porous ceramic "conductivity cell" may furnish a reliable estimate of the soil solution conductivity.

LITERATURE REVIEW

Kemper (1959) was one of the first workers to demonstrate the use of salinity sensors for the in-situ measurement of soil solution EC. His sensor worked in the range of solution concentrations from 0.01 N to 0.5 N and up to -6 atmospheres of soil matric potential. Although successful in many instances, problems arose from the parallel arrangement of the electrodes which involved a relatively high current outside the sensor, and from the dimensions of the probe which resulted in a long response time.

Richards (1966) developed a sensor in which the external field problem was overcome by a different arrangement of the electrodes and by shielding and insulation. His design included a thermistor which provide temperature compensation for the resistance of the electrical conductivity element. The thin (1 mm thick) ceramic plate provided a response time of about one hour for bulk solutions. (Response time is defined as the time required for 63% of the total change in resistance to occur in response to a change in the external concentration). The element could operate within a matric potential range of 0 to -10 atmospheres.

The transducer developed by Enfield and Evans (1969) was constructed of porous glass with platinum electrodes and a thermistor to measure temperature. Repeatability of the sensor was ± 10% in a solution conductivity range of 0 to 20 mmho cm^{-1} at 25°C, operated over the field moisture range, and the time response in aqueous solutions was less than 2 hours.

Reicosky, Millington, and Peters (1970) designed and constructed a sensor in which the sensing element consisted of a Plexiglass core and inner and outer platinum electrodes separated by a sleeve of porous polyvinyl chloride, encased in a ceramic tube. Temperature compensation was also provided by a thermistor resistance network. The sensor was limited to a range from 0 to -0.65 bars of water potential. Response time in free solutions was about one hour and the calibration of sensors remained stable over periods of weeks.

Oster and Ingvalson (1967) modified the Richard's salinity sensor by covering the face electrode with a thin layer of ceramic which prevented dislodgement of the electrode and improved the stability of the sensor. They concluded that the accuracy of salinity sensor measurements in a Pachappa sandy loam soil -- pepper plant system was ± 0.5 mmho cm^{-1} throughout irrigation and drying cycles. The behavior was as good under conditions of low (-7 bars) as well as high matric potentials (saturation). However, Ingvalson et al. (1970), working with the same type of units, showed that sensor conductance was significantly affected when the soil-water matric potential was below -2 bars, although a correction could be made if the change in calibration with matric potential was known. For the same sensors, Oster and Willardson (1971) concluded that 85% of the units used in their experiments were stable and performed satisfactorily for at least 1.5 years with an estimated accuracy of ± 0.6 mmho cm^{-1}.

From these studies we can deduce that despite the important contributions made by these workers, some questions still remain unsolved. The use of sensors to measure soil salinity in-situ is becoming increasingly popular for laboratory and field research [Oster

et al. (1968), Rhoades (1972), Oster and McNeal (1971), Todd and Kemper (1972)]. Also, it is apparent that the use of reliable sensors by growers for evaluating the salinity of their soils on a routine basis could become an important management practice.

For these reasons, the present investigation was undertaken to elucidate further the reliability and limitations of presently available commercial salinity sensors.

MATERIALS

A. Description of Sensor and Salinity Bridge

The salinity sensor (SS) commercially available from Soil Moisture Equipment Corporation (Santa Barbara, California) is that described by Richards (1966) with minor modifications. Figure 1 shows the two commercial types of SS and a cross section view of one of them (cat. No. 5000 A[1/]). Cat. No. 5100-A is of the same design as number 5000-A except that it does not have the spring loading feature and the cable comes out coaxially from the end of the sensor. Both types are designed for use with a salinity bridge (Soil Moisture cat. No. 5500, see description below) in such a way that they provide a direct read-out of soil solution conductivity in millimhos cm^{-1} automatically corrected to the standard temperature of 25°C.

The sensor incorporates the conductance element exposed at one end of the sensor with a thermistor just behind the conductance element. The assembly is encapsulated except for the exposed ceramic surface to produce a permanently sealed unit. The electrical cable from the sensor is a four-conductor cable. Each conductor in the cable is #27 gauge, stranded copper wire with PVC insulation. The four separate conductors are encased in a heavy, black polyethylene jacket which enters the inner area of the sensor and is sealed to it with epoxy resin. The opposite end of the cable is potted into a polarized plug for direct connection to the salinity bridge.

1/ The No. 5000A, 5100A are catalogue number designations of Soil Moisture Equipment Co.

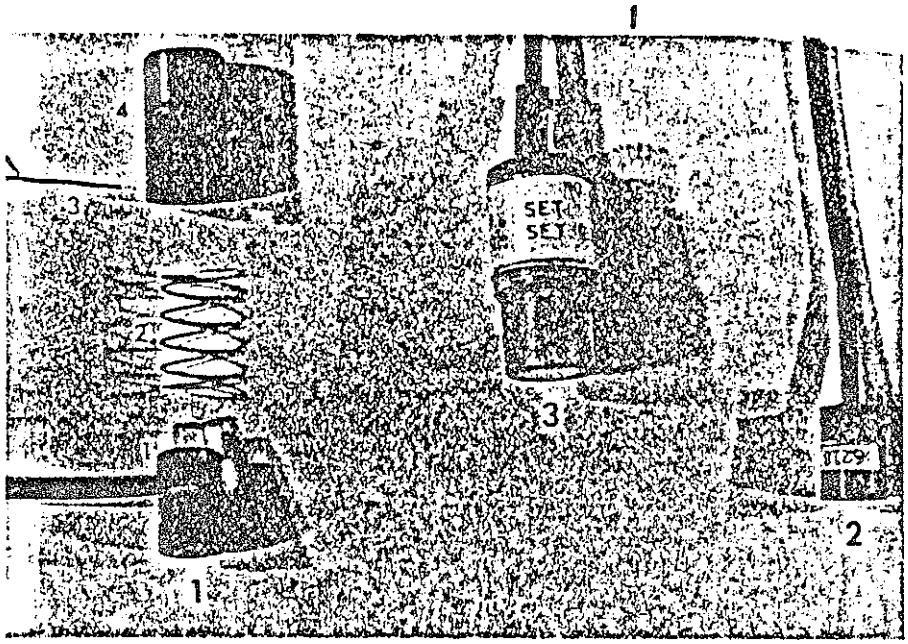

1: Sensor catalog No. 5000A

1 - Inner assembly

2 - Spring

3 - Release pin

4 - Housing

2: Sensor catalog No. 5100A

3: Polarized plug

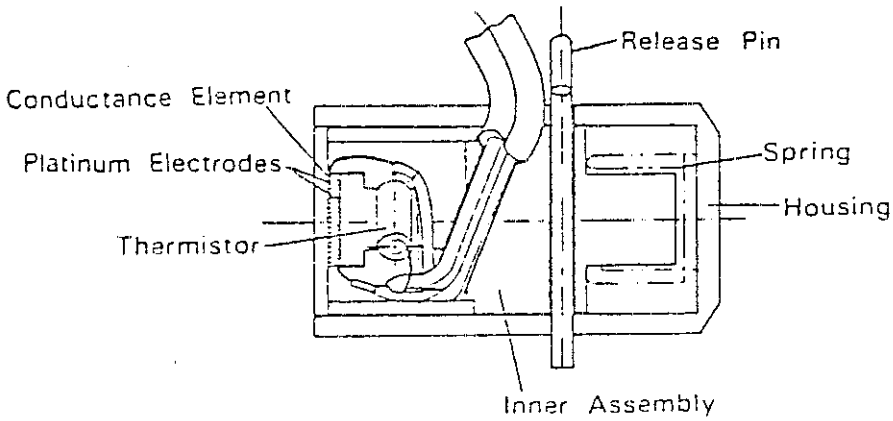

Figure 1. An example of soil salinity sensors made by Soil Moisture Equipment Corporation (Santa Barbara, California).

The conductance element is made of an extremely fine textured, porous ceramic round disc with a cross sectional area of 0.32 cm^2. Two fine mesh platinum electrodes of the same area are fired into the ceramic and spaced 1 mm apart.

The thermistor incorporated into the sensor has a resistance of 2,000 ohms ± 10% at 25°C, and changes approximately 3.9% per °C. By reading separately the resistance of the thermistor, one can readily determine the temperature of the sensor in the range between 0 and 40°C.

The salinity bridge is a 1,000 Hertz, solid state, sine wave AC resistance bridge. The bridge makes it possible to directly read soil solution conductivity in millimhos cm^{-1} at 25°C. It also provides a separate scale for resistance readings.

Figure 2 shows the apparatus and diagram of the bridge circuit. Once the Intercept Setting dial and the Slope-Thermistor Setting dial resistance values are set according to the manufacturer's or other experimental calibrations, the on-off switch is pushed down to energize the circuit and the Read-Out Dial is moved until the pointer of the galvanometer is on the null point. The inner conductivity scale of the Read-Out Dial corresponds to the conductivity of the measured solution corrected to 25°C.

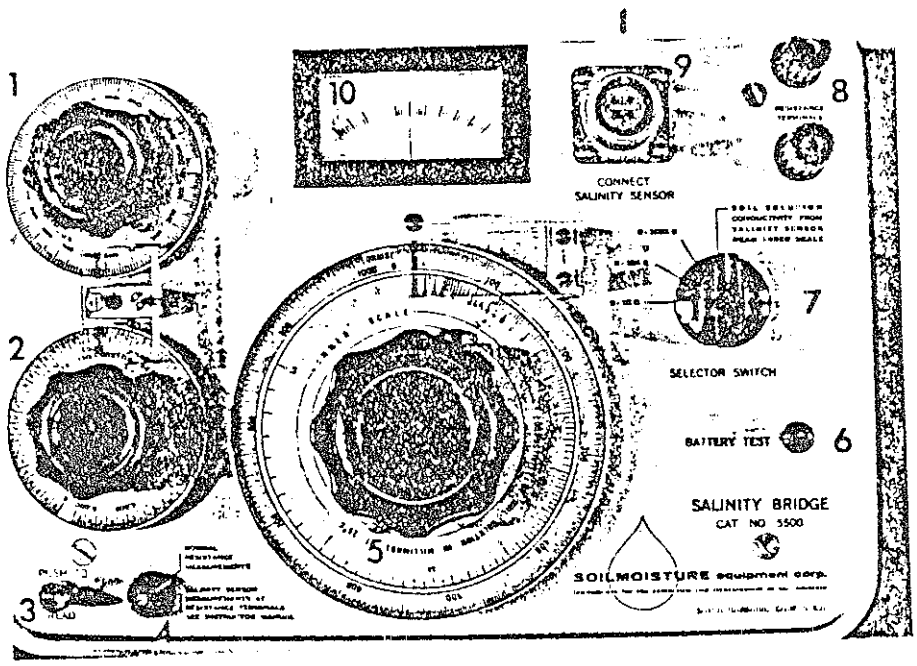

1. Intercept setting dial
2. Slope-thermistor setting dial
3. On-off switch
4. Terminal resistance switch
5. Read-out dial
6. Battery test switch
7. Selector switch for resistance range
8. Resistance terminals
9. Receptacle to accept SS plugs
10. Galvanometer

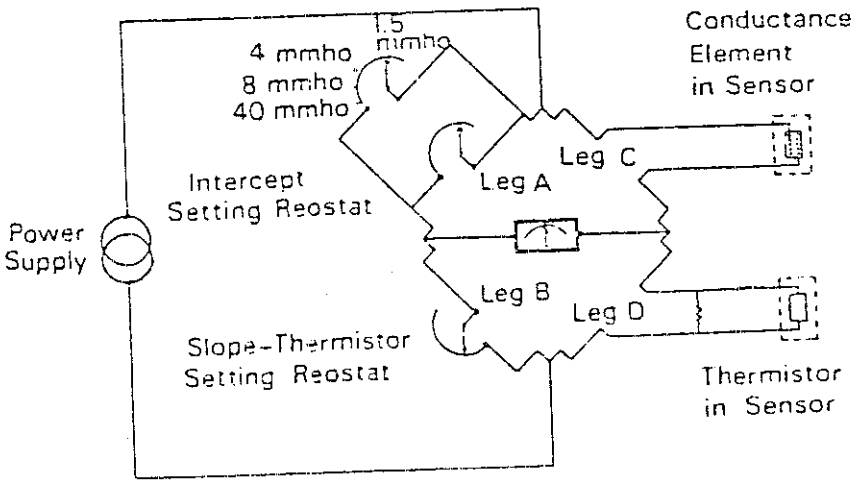

Figure 2. Salinity bridge and bridge circuit diagram made by Soil Moisture Equipment Corporation (Santa Barbara, California).

B. Porous Media

Different porous media were used in several experiments so that the response of salinity sensors to different situations could be determined.

1. Montmorillonite: Finely ground standard Wyoming Bentonite (American Colloid Company, Chicago, Illinois). After separation of the < 0.2 μ fraction, X-ray diffraction patterns were taken in order to detect impurities. The absence of others layered silicates in the sample was confirmed by analyzing the X-ray scan. The reported CEC was 1.1 meq gm^{-1}.

2. Kaolinite: Finely ground Virginia Kaolinite. The absence of others layered silicates in this sample was shown by X-ray diffraction analysis. The reported CEC was 0.05 meq gm^{-1}.

3. Resin: Bio•Rex 70 cation exchange resin, Na-saturated, with an exchange capacity of 10.2 meq gm^{-1} was obtained from Bio-Rad Laboratories (Richmond, California).

4. Sand: pure, uniform particle size sand. Figure 15 shows the soil water characteristic curve.

5. Yolo Loam: surface soil taken from the UCD Campbell Tract field experimental station was air-dried and sieved through a 2 mm square-mesh screen. The measured EC of the saturation extract was 0.8 mmho cm^{-1}, and the CEC was 0.24 meq gm^{-1}. The particle size analysis by sedimentation gave 27.7% sand, 47.2% silt and 25.1% clay. After separation of the < 0.2 μ fraction by methods of M. L. Jackson (1974), the X-ray analysis indicate montmorillonite, vermiculite, mica and kaolinite as the predominant clay minerals. Figure 15 shows the soil water characteristic curve.

Preparation of homoionic systems

Na-saturated samples of various concentration levels were prepared by adding NaCl solutions of known concentrations and stirring. After the sample had settled, the supernatant liquid was decanted off and discarded. The procedure was repeated twice more and samples were kept saturated until used in the experiments.

C. Design and Construction of Columns

The columns (15 cm. in diameter by 14 cm. in height) were constructed from acrylic plastic with 0.2 cm thick walls. Two holes, 2 cm in diameter and 8 holes of the same diameter were made at 4 cm and 9 cm, respectively, from the top of the column for installation of instruments. The top was sealed with a 1 cm thick acrylic plate attached to the column with 4 screws, so that the whole system was capable of holding moderate pressures needed to achieve constant fluxes for the "time response" experiment. Evaporation was also prevented by this procedure.

D. Design and Construction of Suction Probes

Suction probes have been used as sampling devices for many years (Briggs and McCall, 1904). Basically, the sampler consists of a porous ceramic cup or a porous filter cylinder connected to a vacuum system and receiver or collector. The receiver collects a sample of soil water when the vacuum in the sampler exceeds the adjacent soil matric potential.

Important limitations of the suction probe are that extraction of the soil water is possible only for soil matric potentials somewhat higher than -1 bar (Reeve and Doering, 1965), and that it samples a particular partial volume of the total soil solution. Although this has been interpreted as sampling bias - and therefore as a limitation - it might be only because it has not been properly evaluated.

Figure 3 shows a drawing of the apparatus for extracting soil solution. Table 1 summarizes some measured and reported characteristics and properties of the filter cylinder P-10-C, (Coors Porcelain Company, Golden, Colorado) used for extraction.

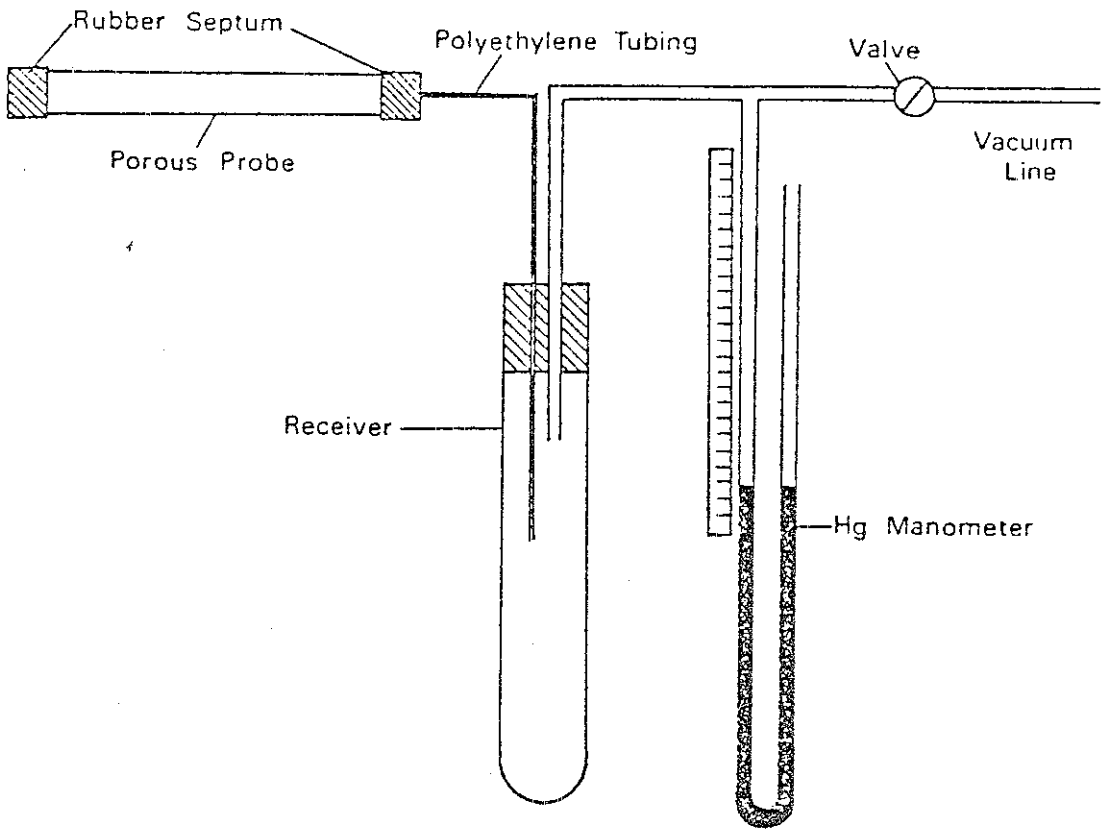

Figure 3. A drawing of the apparatus for extracting soil solution.

Table 1. Properties of Coors Porous Filter Cylinder P-10-C

Length (mm)	100
Diameter (mm)	10
Wall thickness (mm)	2.5
Central cavity volume (cm^3)	1.6
Water retention in the wall (cm^3)	1.4
Pore diameter (microns)	7-10.5
Absorption %	26.1
Bubbling pressure (bars)	0.3-0.4
Rate of flow (ml H_2O/sec/in^2 at 20 psi head)	1.7-2.4

E. Modification of the Pressure Plate Apparatus

A 15-bar ceramic plate extractor (Soil Moisture Equipment Co., Santa Barbara, California) was modified so that instrument wires could go through the wall without leakage at relatively high pressures (up to 15 bars).

Electrically insulated conductors were screwed through 8 threaded holes in the pressure cell walls. Conductors consisted of threaded plastic plugs each with two threaded holes for installation of screws which conduct electric current through the wall of the pressure cell. The screws were sealed by means of O-rings. Wire leads were attached to both ends of the screws by means of suitable terminals. Three of the 8 conductors had constantan and copper wires, for the installation of soil thermocouple transducers (Wescor Inc., model PT 51-10) used in conjunction with a Dew Point Microvoltmeter model HR-33T (Wescor Inc., Logan, Utah) for water potential measurements by the Dew Point method.

PART I Comparison of the electrical conductivity obtained from salinity sensors, solution extracted by suction probe, and soil extract

Through several of the experiments, assessment of the accuracy and response of the salinity sensors was accomplished by comparing the EC with that obtained from suction probe extracted solutions. In so doing, it was assumed that the solution extracted by suction probes was representative of the actual bulk soil solution. Although it is well known that this is not true in all cases [Kapp (1937), Wolff (1967), Hansen and Harris (1975)], and that adsorption of ions by the ceramic cell (Parker, 1925) and soil matric potential at the time of sampling (Reeve and Doering, 1965) should be considered in many instances, Figure 4A shows that the assumption was realistic under our experimental conditions. The important consideration here is that the solution extracted by suction probe had the same electrical conductivity as that of the corresponding extract (2:5 soil-solution ratio) when the vacuum applied was such that the sampling period was short (on the order of minutes). For relatively low vacuum applications and large sampling periods (hours), it is apparent that the electrical conductivity of the solution extracted by suction probe could increase, due to evaporation of the extracted solution in the collector. This was the case for the Yolo loam soil, for which more than 4 hours were necessary to get enough solution for the electrical conductivity measurement at the vacuum level of 0.2 bars (Figure 4B). Therefore, according to this result, and following recommendations by Hansen and Harris (1975), a relatively high constant vacuum (0.8 bars) was used for all samples.

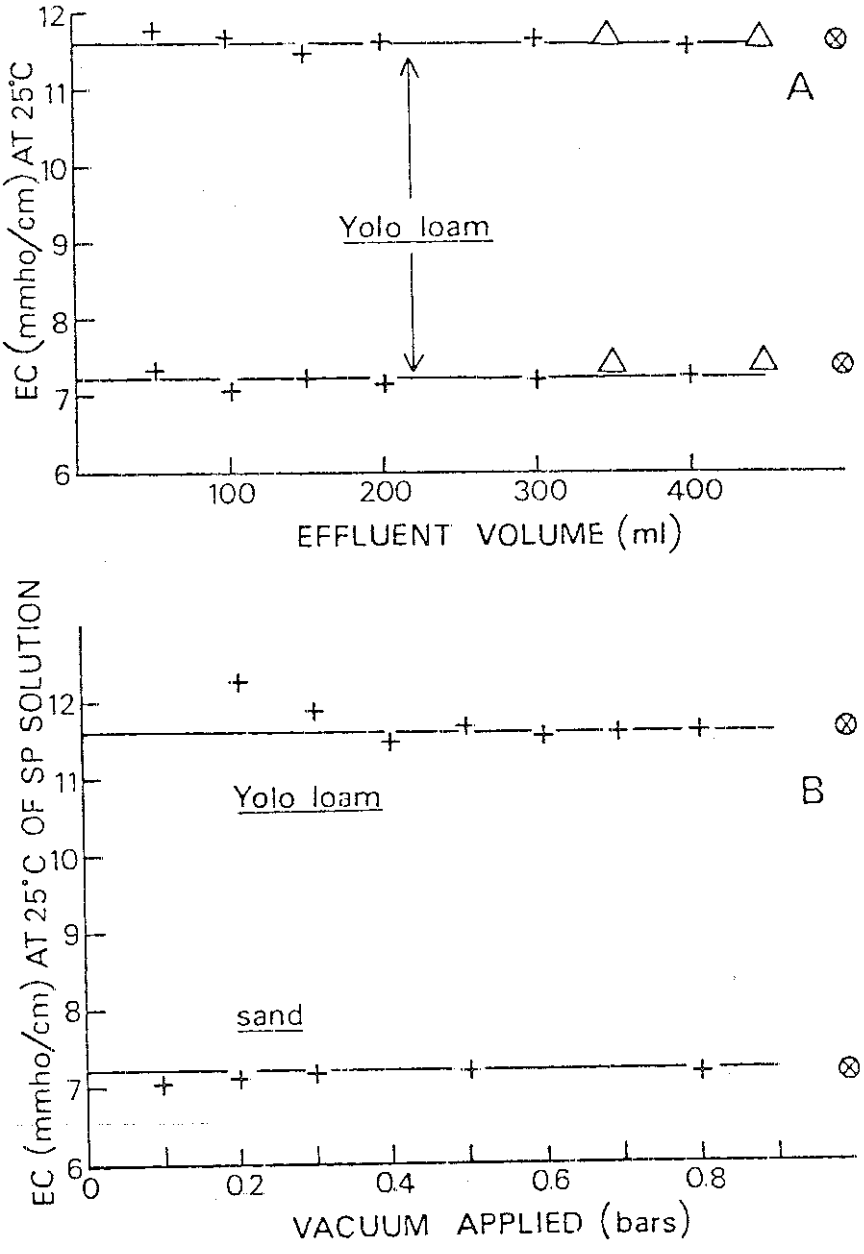

Figure 4. A - Comparison of the EC obtained from salinity sensors (Δ), solution extracted by suction probe (+), and soil extract (⊗). The solid line is the imposed EC.

B - Influence of the vacuum applied on the solution extracted by suction probe (+). The solid line is the imposed EC.

PART II. Calibration of sensors

A. Procedure

Calibration in solution

The sensors were calibrated in solutions of equivalent amounts of calcium and sodium chloride. In making the solutions, equivalent amounts of calcium and sodium chloride were weighed out and dissolved in distilled water to make up the strongest solution desired. Portions of the strong solution were diluted to produce the less concentrated solutions. By this procedure, four solutions were prepared in the range of 2 to 25 mmho cm^{-1}.

A standard conductivity cell together with the salinity bridge described above was used to accurately determine the EC of the final set of calibrating solutions. A conventional alternating current wheatstone bridge was also intermittently used for comparison. The conductivity cell was periodically calibrated with a standard 0.01 N KCl solution. Results of these checks on the conductivity cell are presented in Figure 5 and Table 2. Table 2 shows that the cell constant was relatively stable over a range of temperature for about a year. Data on the relationship between solution conductivity and concentration of ions, and temperature factors (Ft) for adjusting resistance and conductivity data corresponding to the temperature as measured by the sensor thermistors to the standard temperature of 25°C were taken from the USDA Handbook 60 (U.S. Salinity Laboratory Staff, 1954).

The sensors were immersed in the strongest calibrating solution for a period of 10 days in order to minimize entrapped air from the pores of

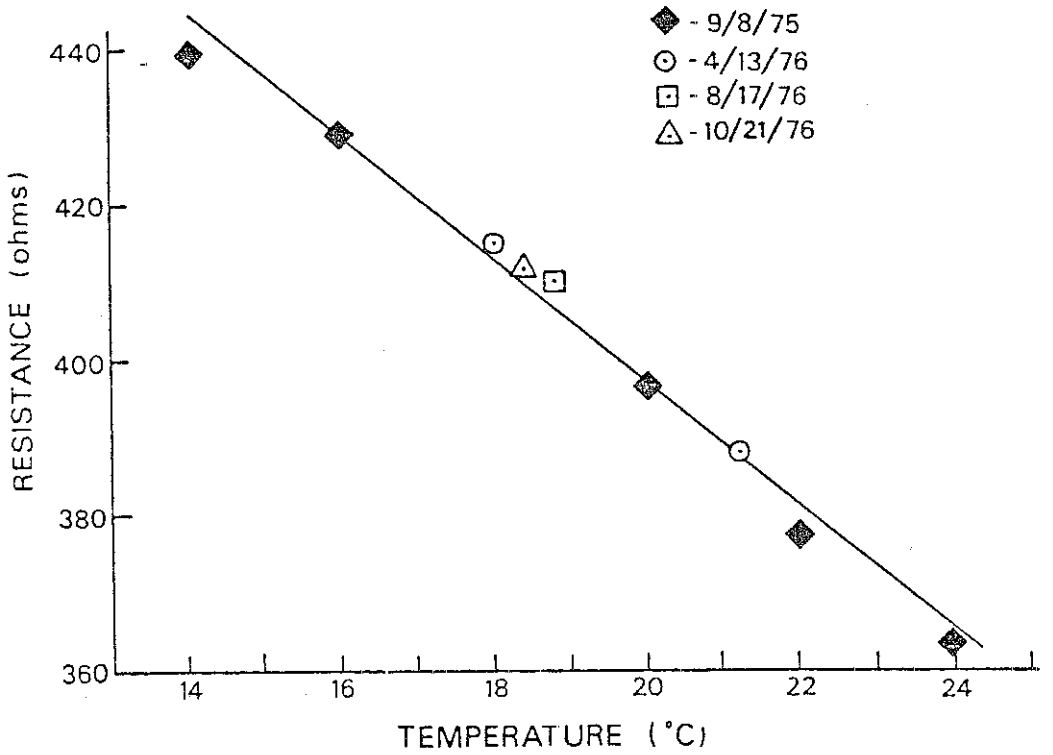

Figure 5. Conductivity cell resistance as a function of temperature of 0.01 N KCl solution.

Table 2. Conductivity cell calibration. Stability of the cell constant over the range 14 to 24°C during one year of operation.

Date	R_T (ohms)	Temp (°C)	F_t	R_{25} (ohms)	K_{cell}
9/8/75	363	24	1.020	355.8	0.502
	378	22	1.064	355.6	0.502
	397	20	1.112	357.0	0.504
	429	16	1.218	352.2	0.497
	440	14	1.277	344.6	0.488
4/13/76	388	21.2	1.085	357.7	0.505
	415	18.0	1.163	356.8	0.504
8/17/76	410	18.8	1.142	359.0	0.507
10/21/76	412	18.4	1.152	357.7	0.505

$K_{cell} = EC_{25} \times R_{25}$

KCl 0.01 N = 0.0014118 mhos cm^{-1} (25°C)

$R_{25} = R_T/F_t$

F_t values from USDA Handbook No. 60

the conductance element. Once equilibrium was attained, readings of the conductance element resistance, thermistor resistance and sensor electrical conductivity were taken with the salinity bridge. The EC of the calibrating solution was obtained immediately thereafter with the conductivity cell. After readings had been completed in the solution of largest concentration, the sensors were removed from the flask. The excess solution clinging to the sensor was removed with absorbent tissue, and the sensors placed immediately in the solution of next lower concentration. After equilibrium - which usually took 1 or 2 days -, readings were taken as described above. The process was repeated for each calibrating solution. Care was taken to minimize evaporation by covering the flask with parafilm paper. A relatively constant temperature was attained by placing the flasks in a water bath in a constant temperature room (19.0 ± 1°C).

To adjust the resistance value of the conductance element to 25°C, it was divided by the temperature factor (USDA, Handbook 60, Table 15) corresponding to the average temperature measured by the sensor thermistor. The conductance of the element in millimhos was determined by dividing the resistance in ohms at 25°C into 1000. The conductance value of the sensor at 25°C in each of the calibrating solutions was then plotted on a graph against the EC of the solutions at 25°C. The calibration curve is a straight line in the range from 0.5 through 30 mmhos cm^{-1}. The intercept and slope values of this line are characteristic of each sensor and are used to obtain the Intercept setting and the Thermistor-Slope setting on the salinity bridge. Instructions are given in the salinity sensor operating instructions for the calculation of these settings.

Influence of entrapped air in the conductance element on calibration

A set of six sensors were used to study the influence of air in the conductance element on the calibration. Three different initial conditions were imposed: (i) sensors ten days in solution, (ii) sensors wet under vacuum and (iii) sensors air-dry, and the calibration made as outlined above, omitting the 10 days in solution for cases (ii) and (iii).

Stability of the calibration

After calibration, the sensors were placed in a 1 mmho cm^{-1} solution for three days (in order to prevent large evaporation deposits of salt on the surface of the conductance element), removed from the solution and allowed to air-dry. Fourteen months later, after being used in other experiments, the sensors were recalibrated as outlined above and the results statistically compared with the previous calibration data.

Hysteresis of the calibration

The sensors were checked for hysteretic behavior by making two successive calibrations, one from the weakest to the strongest solution and the other in the opposite direction. The results were analyzed statistically.

Calibration in soil

Basically the procedure is the same as that described above for calibration of sensors in bulk solution, except that four of the columns described in "Materials" (p. 13) were filled with Yolo loam soil, equilibrated at four different solution concentrations in the range from

2 to 14 mmho cm^{-1}, and used instead of the solution itself. After determining that the outflow solution and the solution extracted by suction probe had the same EC as that of the influent solution, drainage of the column was stopped, and salinity sensor readings were taken at equilibrium.

B. Results and Discussion

Influence of entrapped air in the conductance element on calibration

Table 3 gives the regression analysis of the calibration data for two of the sensors studied, and figure 6 shows their calibration curves. Of the six sensors examined, four showed behavior "A" and the rest behavior "B".

From these limited data, it is apparent that entrapped air in the pores of the sensor ceramic results in higher than normal resistance readings. Behavior "A" was considered to be the normal response of well-made sensors to the presence of air in the ceramic: for the dry sensor the first reading (largest ECs) resulted in lower than normal conductance values but as the calibration proceeded, dissolution of air in the ceramic occurred, and the final readings were almost identical to those obtained in the two other treatments. Also, it is noted that both the wet under vacuum and 10 days in solution treatments gave close results, although the wet under vacuum correlation coefficient was lower than that of the 10 days in solution treatment.

The "abnormal" behavior of the sensor represented in figure 6B can be explained by the presence of stagnant pores in the ceramic. When the sensor was dry, the decrease in conductance values relative to the standard calibration curve (10 days in solution treatment) was persistent

Table 3. Regression analysis of the calibration data for two of the sensors examined for the influence of entrapped air in the conductance element.

Sensor	Treatment	Calibration Curve Cse = A + B ECs*	Correlation coefficient r
A	(i) 10 days in solution	Cse = 0.241 + 0.1281 ECs	1.0000
	(ii) wet under vacuum	Cse = 0.246 + 0.1276 ECs	0.9989
	(iii) dry	Cse = 0.440 + 0.9650 ECs	0.9869
B	(i) 10 days in solution	Cse = 0.240 + 0.0701 ECs	0.9977
	(ii) wet under vacuum	Cse = 0.481 + 0.033 ECs	0.9465
	(iii) dry	Cse = 0.102 + 0.066 ECs	0.9850

* Cse = sensor conductance (mmho) at 25°C, ECs = solution conductivity (mmho cm^{-1}) at 25°C.

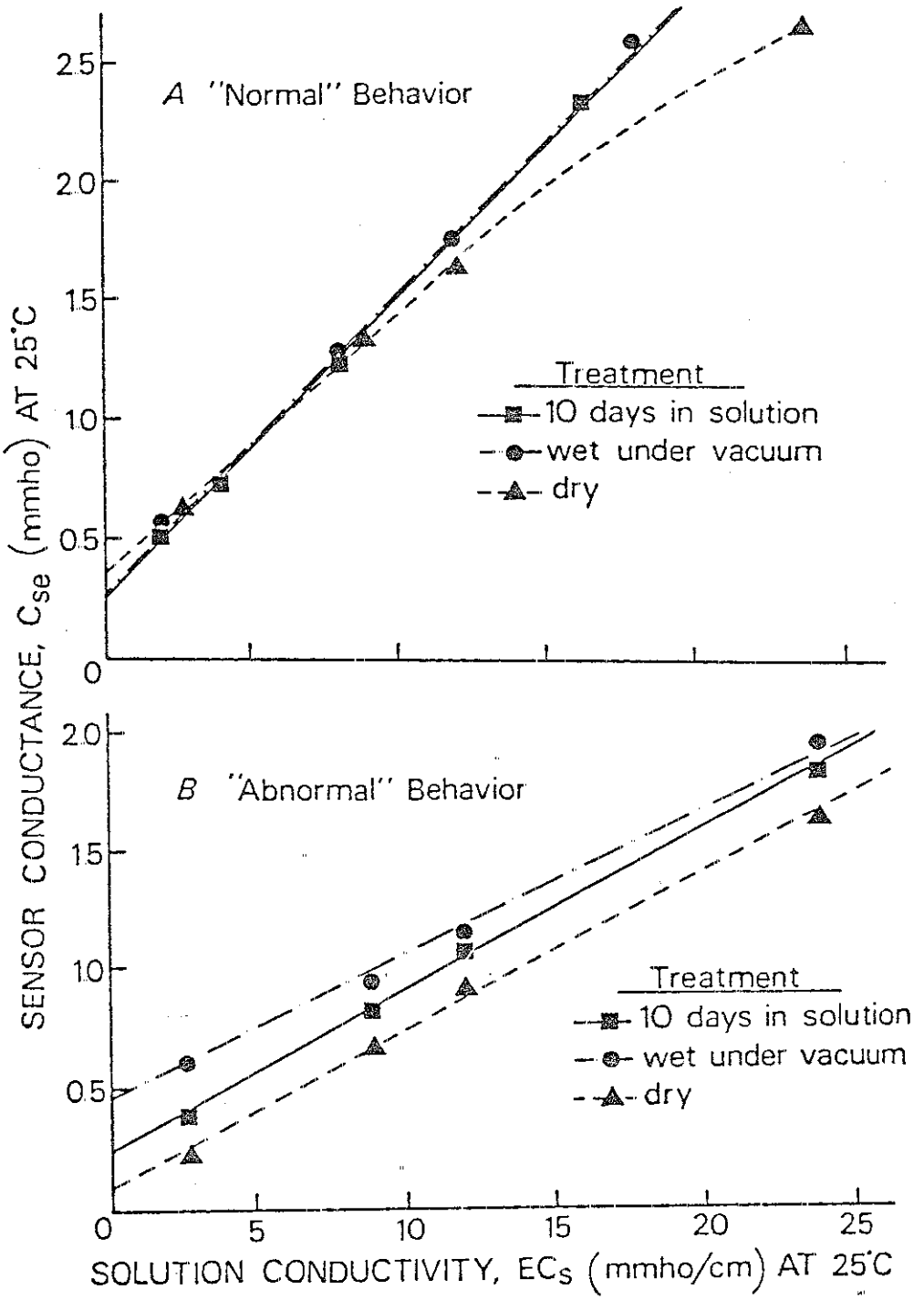

Figure 6. Influence of entrapped air in the conductance element on the calibration.

throughout the calibration range meaning that little dissolution of air occurred. The relatively small decrease in the slope value with a still high correlation coefficient ($r = 0.985$) confirms this hypothesis. On the other hand, when the same sensor was wetted under vacuum, it showed a large decrease in the slope value and a large increase in the intercept or inherent conductance value. This suggests that some pores, which were evacuated by the applied vacuum and became filled with solution of relatively high EC were stagnant. The solution in these pores did not change much during the calibration process so that they imparted a relatively high conductance to the unit, despite the fact that the rest of the pores were in equilibrium with the succeeding less concentrated calibrating solutions.

This result is of practical interest for many field situations because it allows identification of those sensors which upon becoming dry, will change in their calibration characteristics for appreciable time. The fact that this change underestimates EC values is an important consideration, especially when sensors are used for monitoring soil salinity in relation to plant growth.

It is recommended that a test like the one depicted above be made before installation of the units in order to eliminate those behaving like the unit in figure 6B.

Also, the practice of wetting the sensors under vacuum before calibration seems to be inappropriate for practical purposes because the situation more likely to occur in the field is that of most stagnant pores being filled with air, although we should recognize that in soil atmospheres of higher CO_2 content the air will be more readily dissolved.

Stability of calibration

A set of twenty-two sensors were examined for stability of calibration. The first year the sensors were calibrated (cal. 1975b) and the results compared with those given by the manufacturer (cal. 1975a). Table 4 shows that the average slope and intercept values of both calibrations were very similar. Consequently, cal. 1975a was chosen as our point of reference for the study of the shift in calibration of the units with time. Fourteen months later the sensors were recalibrated (cal. 1976) and the results compared with cal. 1975a.

Before further discussion, we should establish the criteria for stability. Oster and Willardson (1971) considered that "sensors had stable calibration characteristics if the calibration curves at different dates were within ±15% of the average calibration curve throughout the range of calibration." In our opinion, this criterion involves some difficulties: (i) by taking the average calibration curve as the reference, the possible shift of the calibration curve is somewhat underestimated, and (ii) to generalize the application of a ±15% change in the calibration curve to all sensors as criterion for stability could give erroneous conclusions.

We consider that a sensor has a stable calibration if the slope and intercept values of the calibration curves at different dates are within ± two times their largest standard deviations.

With this criterion, 23% of the sensors examined were considered to be stable. Of the unstable sensors, 93% showed a typical shift of the calibration curves with an average decrease of 18.9% in the slope and an average increase of 30.9% in the intercept. Figure 7 shows the frequency distributions of the slope and intercept values of the

Table 4. Average calibration curves and correlation coefficients of the twenty two sensors examined for stability of calibration

	Calibration Curve Cse = A + B ECs*	Correlation coefficient r
cal. 1975a	Cse = 0.212 + 0.1008 ECs	0.9994
cal. 1975b	Cse = 0.211 + 0.1023 ECs	0.9972
cal. 1976	Cse = 0.259 + 0.0846 ECs	0.9965

* Cse = sensor conductance (mmho) at 25°C, ECs = solution conductivity (mmho cm^{-1}) at 25°C.

unstable sensors, with the corresponding mean and standard deviations. Figure 8 shows calibration data for one sensor that was judged to be stable (A) and for another (B) which showed the typical deviation mentioned above. The appendix is the regression analysis of individual calibrations 1975a and 1976 performed for each sensor. The calibration equation, correlation coefficient and standard deviation of the intercept and slope values are shown.

In general, for the unstable sensors the difference in intercepts between cal. 1975a and cal. 1976 were close to the ± two times the standard deviation, whereas the difference in slopes were far from this figure. This is somewhat reflected in the average values of the intercept and slope in Figure 10.7.

The reason for the apparent increase of the intercept value was thought to be adsorption of ions on the surfaces of the porous ceramic clay. Precipitation of salts on the surface of the electrodes and probably within the ceramic itself will be mainly responsible for the decrease of the slope value. Thus, after having nine sensors in a 1 N KCl solution for 35 days under continuous stirring, their recalibration showed a tendency toward the original calibration curve (1975a) for four of them. For three sensors the slope of the 1976 calibration remained constant or even decreased (this experiment was done three months later than cal. 1976), and two sensors had a relative increase in the slope values.

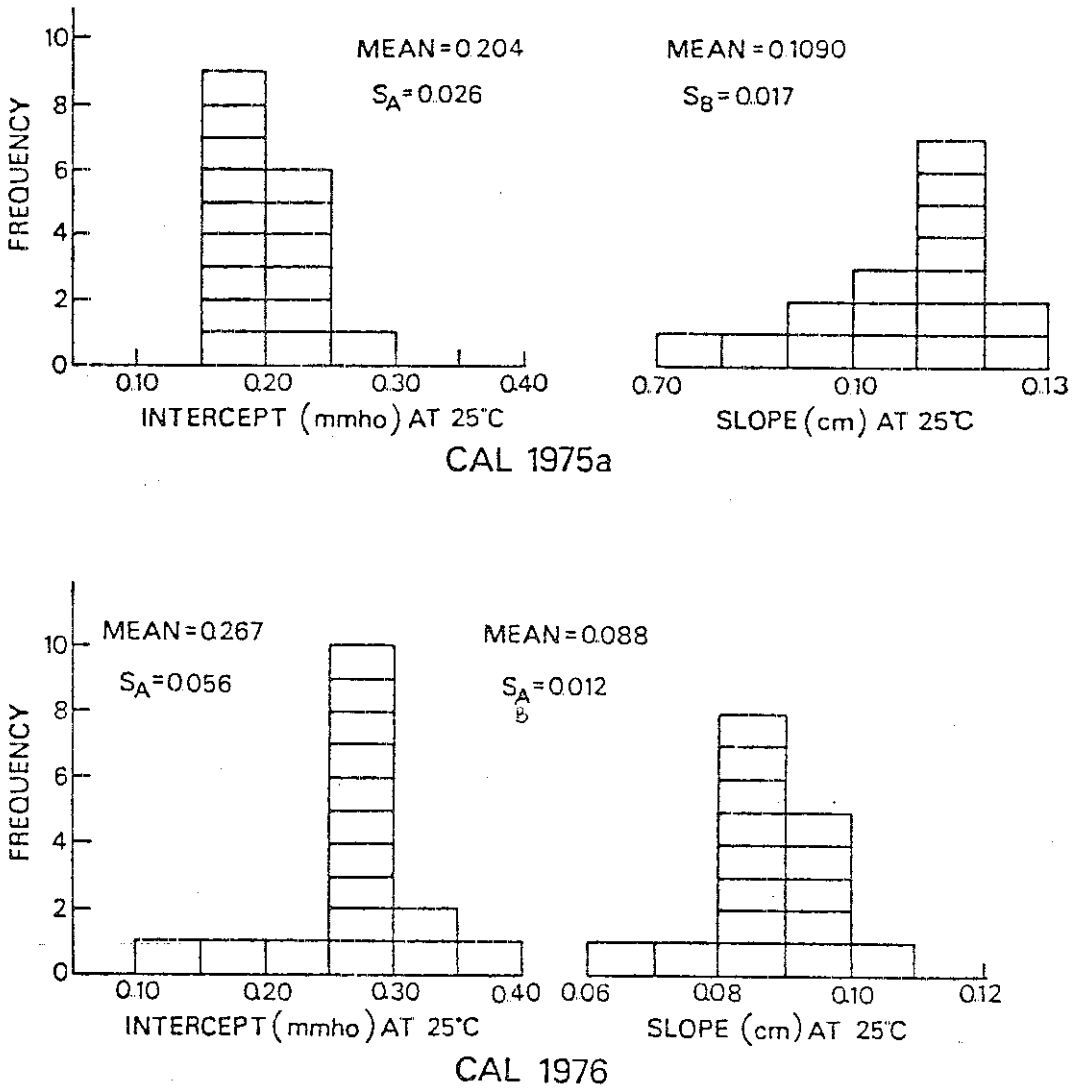

Figure 7. Frequency distributions of the slope and intercept values of the unstable sensors (evaluated for a period of 14 months).

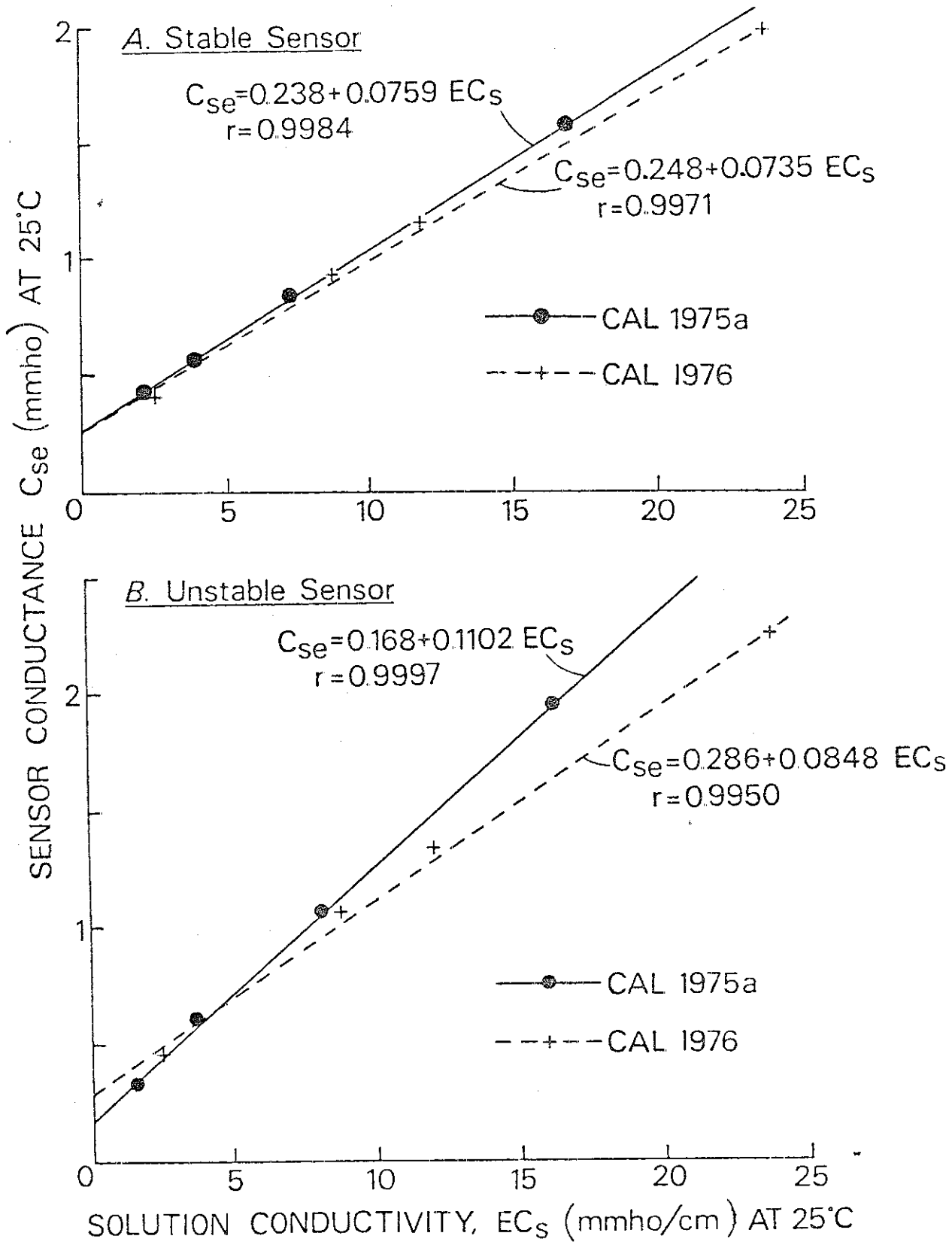

Figure 8. Calibration curves of a stable sensor (A), and a typical unstable sensor (B) (evaluated for a period of 14 months).

Although these limited results are not conclusive, it seems that precipitation of salts is one of the main reasons for this shift in calibration although some other factors should probably be taken into account. If this is the case, we could expect the instability of field installed sensors to be accentuated due to the presence of salts more likely to precipitate in the conductance element (alkaline-earth carbonates, gypsum, etc.), especially under wetting and drying cycles. In that sense, the seriousness of the problem will probably be of less importance in trickle irrigation or high-frequency irrigation systems where the soil water content remains relatively constant.

Due to the typical shift of the calibration curves which appears as a clockwise rotation of the lines with the center of rotation in the region around EC = 4 mmho cm^{-1}, errors produced by the change in calibration were relatively small for this region and increased for increasing EC's. Figure 9 shows the frequency distribution of EC errors involved in the shift of calibration and the mean of these errors at various EC levels.

Although the errors involved at low EC levels are not important for most practical situations, we should consider that, according to the USDA Agriculture Handbook No. 60, a soil is considered to be saline when the EC of the saturation extract is more than 4 mmho cm^{-1} at 25°C. In terms of actual concentration of the soil solution, with which the sensor is in equilibrium, this is about 8 mmho cm^{-1} for the upper end of the field moisture range and about 16 mmho cm^{-1} for the "permanent wilting" point. Therefore, it is apparent that the shift in calibration might be of practical importance for many saline conditions.

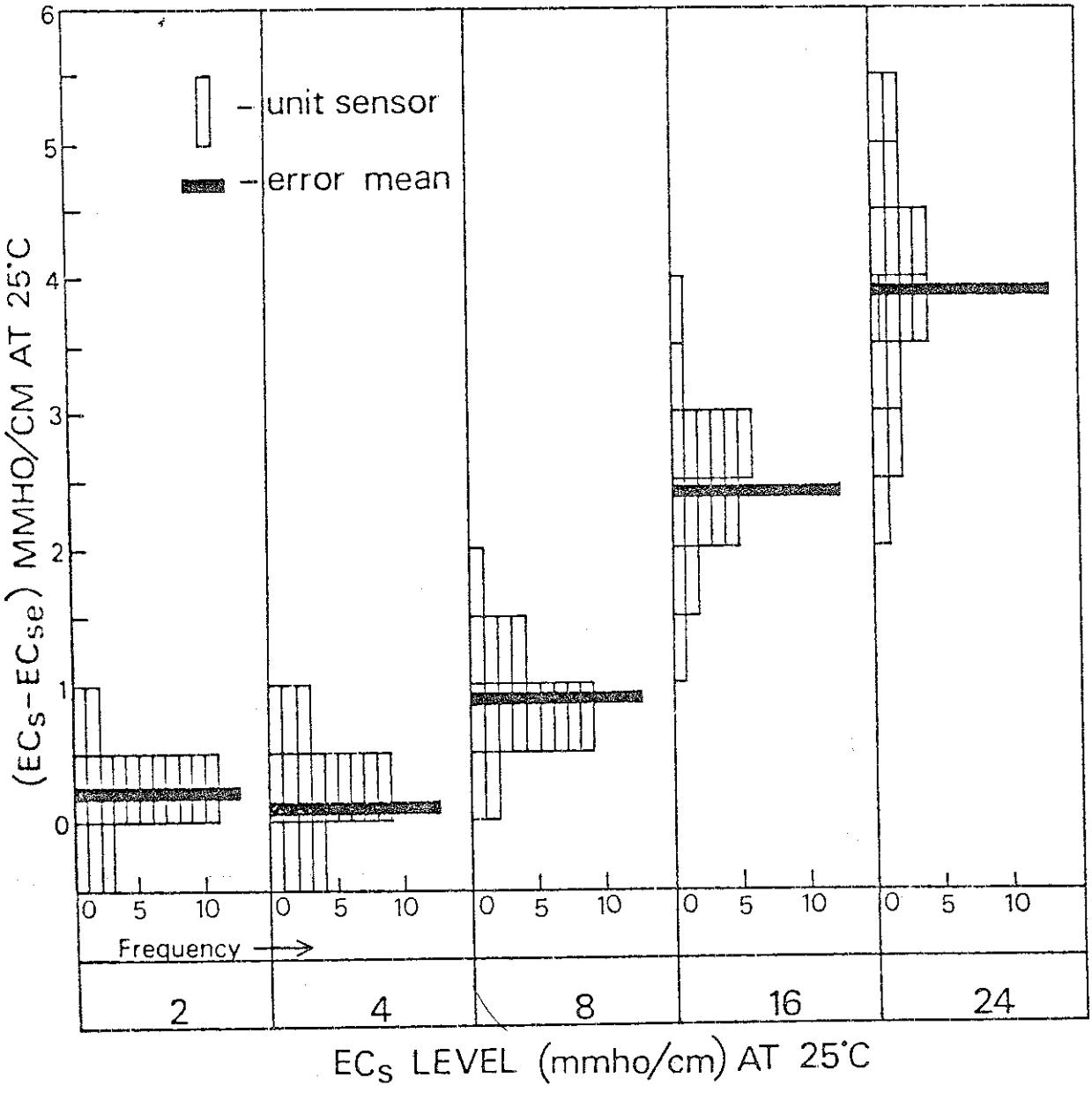

Figure 9. Frequency distributions of electrical conductivity errors at various EC levels involved in the shift of the calibration over a period of 14 months.

With these limited data at hand, a way to correct installed sensors suspected to have become unstable (generally those with unpredictably low EC readings) without removal and recalibration is to correct the sensor conductivity reading to the actual soil water conductivity by means of figure 10. Figure 10 is obtained from the calculated ECs values as

$$EC_1 = \frac{(A_2-A_1)}{B_1} + \frac{B_2}{B_1} EC_2$$

and plotted against actual EC_2. Numbers 1 and 2 refer to average cal 1975a and cal 1976, respectively. The shaded area represents the estimated accuracy of the correction.

Further work should be done to elucidate the importance and progression of the shift in calibration with time. Limited results from sensors calibrated five months after cal. 1976 suggest that those sensors considered to be stable on the basis of previous calibrations showed a tendency toward the typical shift mentioned above, whereas in the unstable sensors calibration shifts have stopped or are greatly reduced.

Oster and Willardson (1971) evaluated the stability of 26 commercial sensors for 1.5 years, during which time 85% were stable. They did not mention how the sensors were kept during this period of time. Using their criteria for stability, we found that only 30% of our sensors were stable for 1.2 years of operation. Kemper (1959) did not find consistent changes in the resistance of the units after three months of operation except in the case of one set of units which was allowed to air-dry in contact with Fort Collins soil. Although his

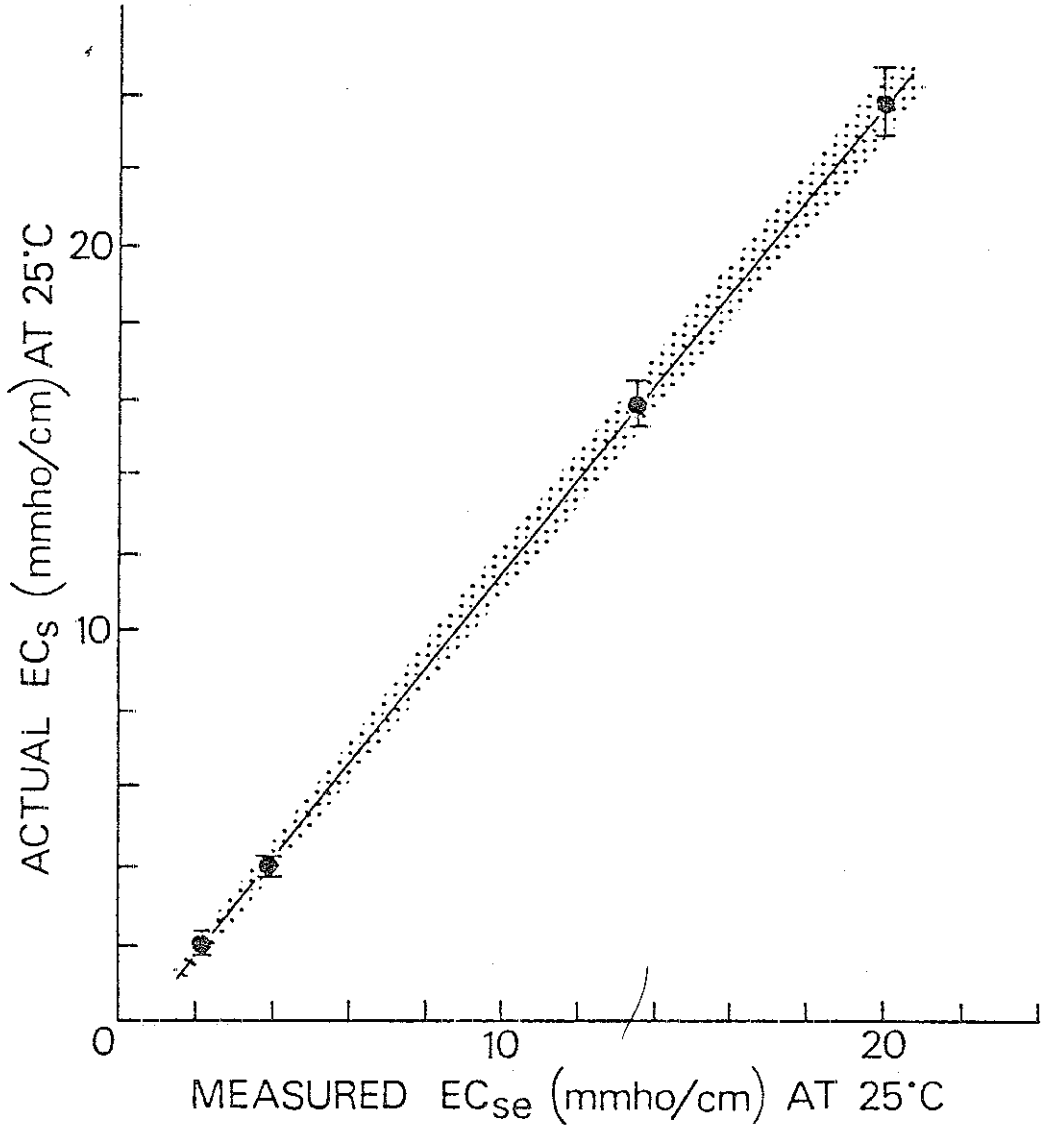

Figure 10. Correction chart for the unstable sensors. Shaded area represents the standard deviation of the mean.

sensors were different in design and construction from the commercial units we used, we should specify that during our experimental work all the units were dry one time or another. We were not able to correlate dryness of sensors with the shift in calibration, but a rigorous analysis of this fact was not performed. However, we should recognize that the drying of sensors will enhance the precipitation of salts in the conductance element, a fact that will be in accordance with our results.

Accuracy of measurement

The accuracy of EC measurements obtained with a calibrated sensor can be estimated from the linear regression analysis of the calibration data. Table 5 shows the average standard deviations and correlation coefficients from regression. The standard deviation from regression S_{y-x} divided by the slope of the calibration line, is an estimate of the standard deviation of EC measured by the sensor. Assuming that a variation of two times the standard deviation can be expected to occur, the accuracy of the EC measured by the units is shown in last column.

From these data, it is apparent that the accuracy of sensors decreased with time. Still, the estimated level of accuracy seems to be satisfactory for most practical needs. However, we should be aware of the fact that these estimates of accuracy are on the basis of the actual calibration curves. It should be recognized that for practical purposes, calibrating the sensors every six months is not a current practice. Thus, the values obtained take into account the change in calibration and do not represent the actual accuracy of the installed sensors. If a regression analysis is performed on all the data from calibrations 1975a

Table 5. Average values of the regression analysis performed on twenty two sensors. The estimated accuracy of the measurement is shown in the last column.

Calibration	Cse = A + B ECs	r	S_{y-x} (mmho)	S_{x-y} (mmho cm^{-1})	Accuracy (mmho cm^{-1})
1975a	Cse = 0.212 + 0.1008 ECs	0.9994	0.016	0.16	± 0.32
1975b	Cse = 0.211 + 0.1023 ECs	0.9972	0.032	0.31	± 0.62
1976	Cse = 0.259 + 0.0846 ECs	0.9965	0.042	0.49	± 0.98
Soil cal 1975	Cse = 0.267 + 0.1004 ECs	0.9749	0.072	0.72	± 1.44

Cse = Y = sensor conductance (mmho) at 25°C

ECs = X = solution EC (mmho cm^{-1}) at 25°C

r = correlation coefficient

S_{y-x} = S_{x-y} B = standard deviation

Accuracy = two times S_{x-y}

and 1976 for each sensor, the corresponding estimated accuracies are (on the average) ±0.71 mmho cm^{-1} for the stable sensors and ±1.92 for the unstable sensors. For illustration, figure 11 shows the regression analysis performed on two of the sensors, one considered to be stable and the other unstable.

Calibration of sensors in soil was performed only at the beginning of the work when cal 1975b was done (table 5). Experimental data indicate that the estimated accuracy (±1.42 mmho cm^{-1}) is conservative. Probably the soil did not achieve true ionic equilibrium, especially at low concentration levels due to the relatively high Mg content of the dry soil. Therefore, this result is questionable.

On the basis of these data we concluded that the estimated accuracy of EC measured by the sensors after more than one year of operation was in the order of ±0.7-0.9 mmho cm^{-1} for the stable and corrected unstable units and around ±2 mmho cm^{-1} for the non-corrected, unstable sensors.

We tried to elucidate the feasibility of using a single calibration curve rather than individual calibration values for sensors of somewhat similar characteristics. The change in calibration characteristics of units with time did not allow us to perform such analysis. Even if it is assumed that the shift in calibration stopped after one year of operation the approach is unrealistic for actual sensors. For illustration, Figure 12 shows the uncertainty of the measurement when the average calibration curve 1976 in Figure 9, Cse = 0.27 + 0.09 ECs was applied to those sensors with intercepts of 0.27 ± 0.1 mmho and slopes of 0.09 ± 0.01 cm.

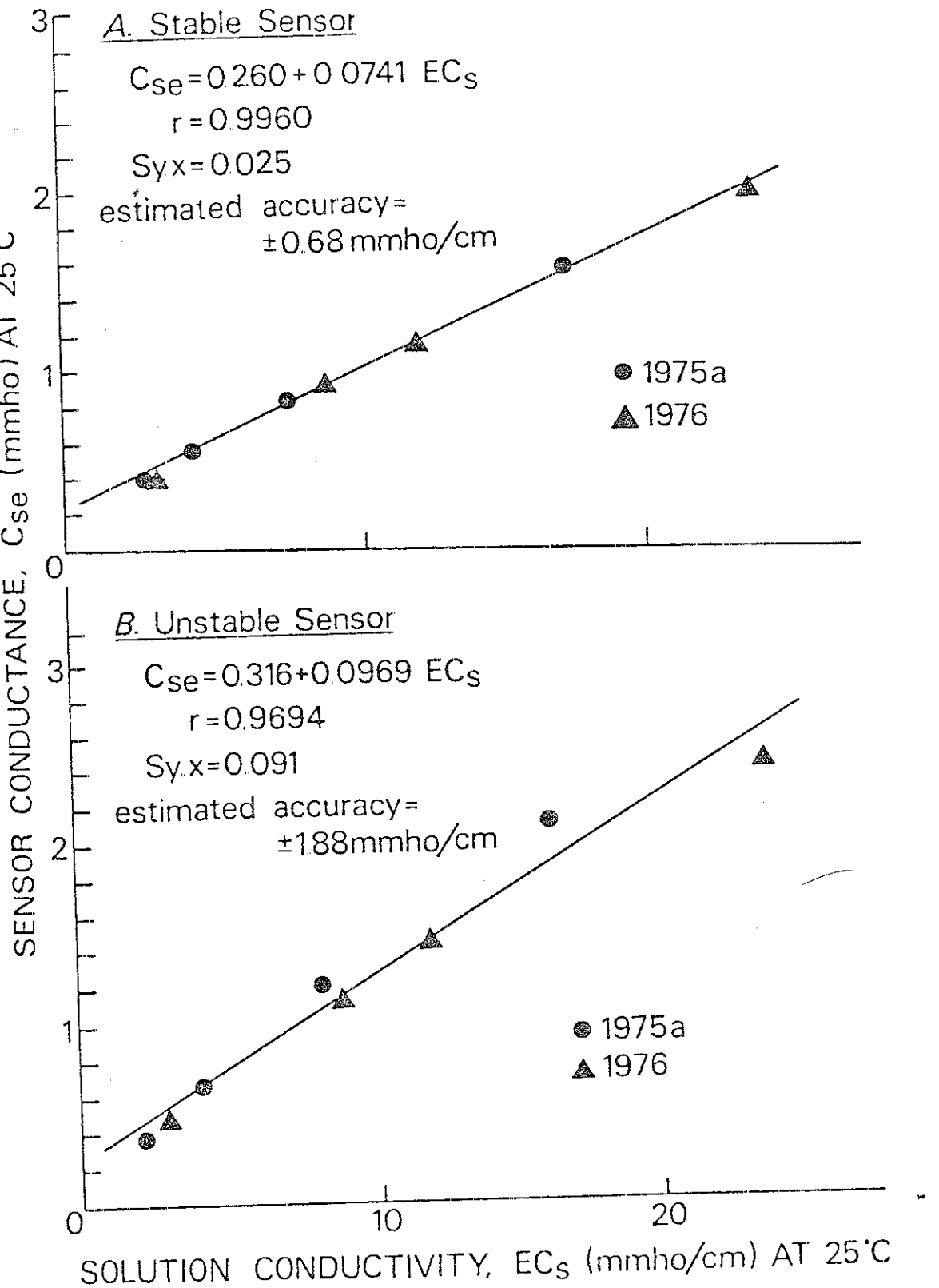

Figure 11. A calibration curve for a stable sensor (A) and an unstable sensor (B) when data points from cal. 1975a and cal. 1976 are considered to best fit one single line.

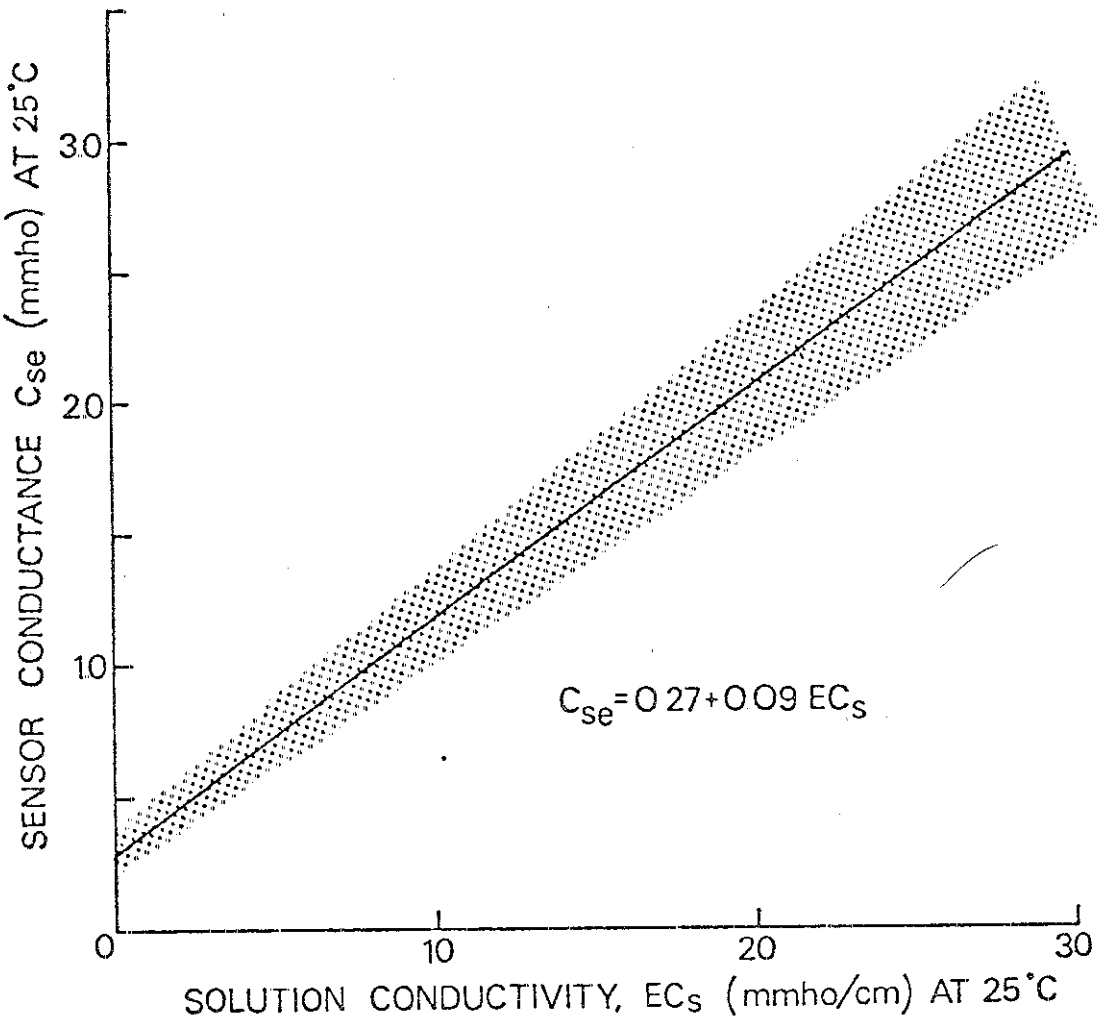

Figure 12. Uncertainty of measurement using a single calibration curve for all sensors of similar characteristics. Shaded area represents the standard deviation of the mean.

Hysteresis of calibration

Six sensors were checked for hysteretic behavior by calibrating them in NaCl solutions. Table 6 shows the regression analysis of the data for individual sensors.

Two of the sensors (No. 4606 and No. 6197) showed a significant increase of their intercept values for case b. Again the reason could be the presence of stagnant pores in the porous ceramic. As expected, the increase of the intercept value is much less than that obtained for those wet under vacuum because here we used the standard method of calibration (10 days in solution treatment) and therefore most of the stagnant pores will be filled with air rather than with solution. The conclusion is that normal sensors show little, if any, hysteresis, whereas those sensors with non-conductive pores show appreciable hysteresis in their calibration curves.

Table 6. Regression analysis of the six sensors examined for hysteretic behavior.

Cse = A + B ECs*	Sensor Number											
	4606		4652		4998		6171		6193		6197	
	a	b	a	b	a	b	a	b	a	b	a	b
A	.260	.272	.241	.242	.306	.298	.448	.440	.431	.429	.458	.477
B	.0633	.0630	.0703	.0705	.0764	.0773	.1206	.1215	.1100	.1107	.1219	.1216
$r^{\dagger}$	.997	.995	.999	.998	.998	.997	.999	.998	.999	.998	1.000	.999

a = calibration from low to high concentrations

b = calibration from high to low concentrations

* Cse = sensor conductance (mmho) at 25°C; ECs = solution conductivity (mmho cm^{-1}) at 25°C

† r = correlation coefficient

PART III. Time response of sensors

A. Procedure

Time response in solution

Three experiments were conducted for three different initial conditions. For the first experiment a set of 12 sensors were placed in a solution of known EC for ten days to assure true equilibrium. The sensors were then placed in another solution and sensor readings were periodically recorded until equilibrium was reached.

The procedure was repeated for several different salt solutions of known EC, in both an increasing and decreasing direction of solution concentrations.

For the second and third experiments the sensors were first allowed to air-dry or wet under vacuum and then placed in solution. The time needed to achieve equilibrium in the new, imposed concentration was recorded.

Time response in porous media

Time response of salinity sensors in porous media was determined by two procedures:

(i) After equilibration of the sensors in a 0.5 mmho cm^{-1} NaCl solution for ten days, a set of six sensors was placed in a sand column and another set in Yolo loam column which had been previously equilibrated with a NaCl solution of known concentration. Two air-dry sensors were also placed at the same time in each column. Sensor readings were periodically taken until equilibrium was reached. The sensors were then placed in the next soil column and the procedure

repeated. Time response was also checked for sensors in sand and Yolo loam soils previously equilibrated at matric potentials of -0.1 and -0.4 bars.

(ii) Figure 13 shows the apparatus of an experiment in which NaCl solutions of increasing concentrations were consecutively forced at a constant flow rate (cm/hr) through four porous media: cationic resin, sand-Kaolinite (2:1 by weight), sand and Yolo loam. Once these porous media attained a dynamic equilibrium with the NaCl solution of lower concentration, the next concentrated solution was added.

Sensor readings and suction probe extractions were periodically made until achievement of a new "equilibrium". The procedure was continued for the next concentrated NaCl solution. After the system equilibrated with the strongest solution, the NaCl solution of lowest concentration was forced again through the column. Constant fluxes were attained with a syringe pump connected to an electronic motor speed control (model 4X796 of Dayton Electric Manufacturing Co., Chicago).

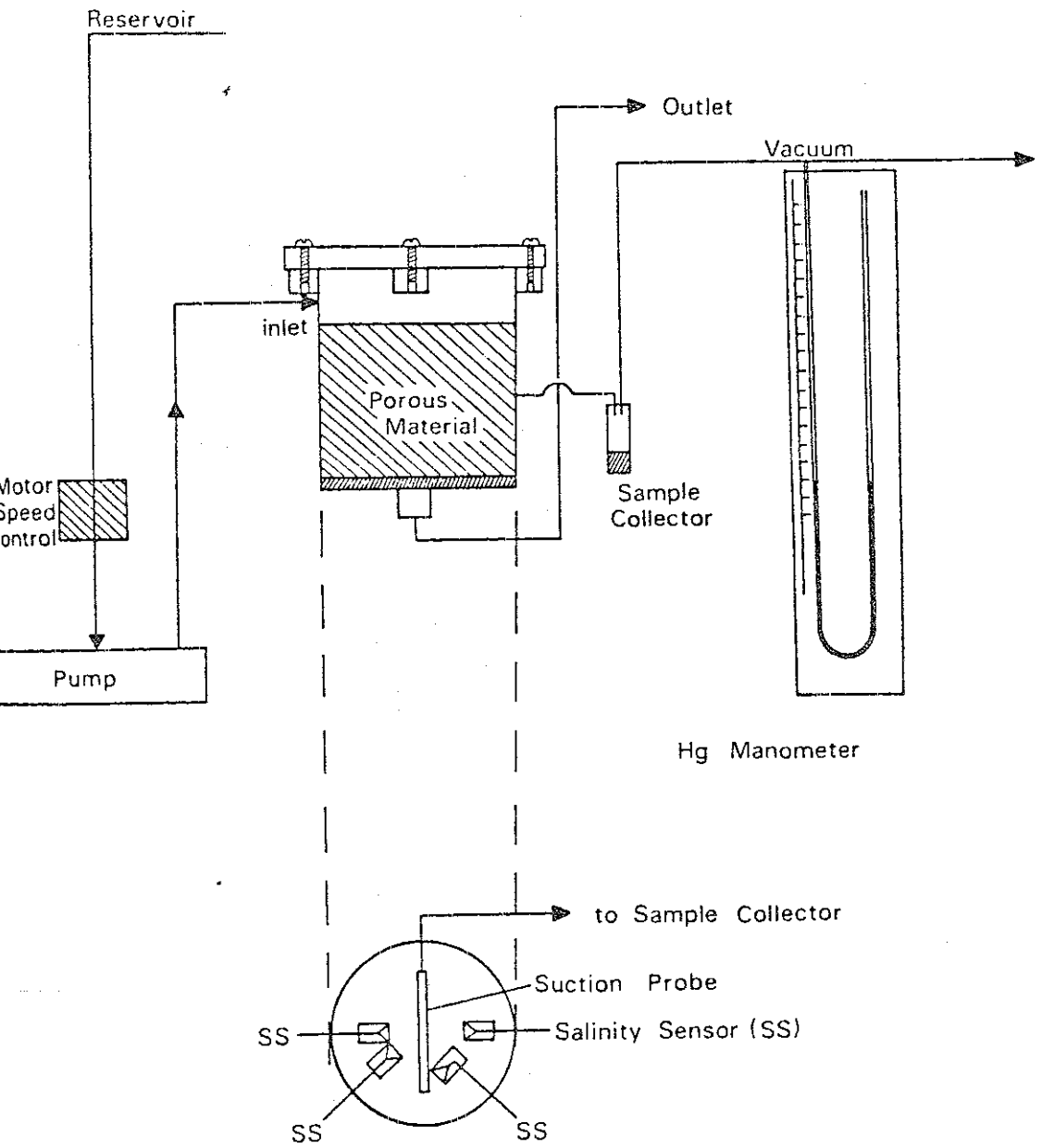

Figure 13. Experimental apparatus used to measure the response of salinity sensors and suction probes to solutions of various concentrations.

B. Results and Discussion

Table 7 is a summary of the results obtained from time response experiments, part (i). The last column of the table indicates the number of sensors used in each experiment, with the number of replications in parenthesis. Sensors in porous media at Ψ_m = -0.4 bars never attained the conductivity value of the soil water; the range of equilibrium values as percent of change expected with normal response are given in parenthesis in the third column of the table. Time response of experiments #1, 2 and 3 was checked for four different NaCl solution concentrations in the range from 2 to 24 mmho cm^{-1}. No significant differences in time response were found in general between these solutions for each individual sensor. As an illustration, figure 14 shows the time response for a unit which is representative of the average results obtained in solution.

Time response refers to the time required for sensors to reach 63% (or 100% as indicated) of equilibrium response when moving the sensors from one concentration level to another.

The percent change at time t is obtained from

$$\% \text{ change at time } t = 100 \times (EC_o - EC_t)(EC_o - EC_f)^{-1}$$

where EC_o = sensor electrical conductivity (mmho cm^{-1}) at time zero

EC_t = sensor electrical conductivity (mmho cm^{-1}) at time t

EC_f = sensor electrical conductivity (mmho cm^{-1}) at final equilibrium

Table 7. Time response of sensors. Numbers in parentheses in last column indicate replications.

A - 10 days in solution sensor

#	time response in	63% of total change mean ± stand. dev. (hrs)	100% change mean ± stand. dev. (hrs)	No. of sensors
1	solution	2.8 ± 0.60	14.6 ± 1.9	12 (1)
2	saturated sand	3.6 ± 1.60	29 ± 3.2	6 (1)
3	saturated Yolo loam	3.5 ± 1.90	24 ± 8.8	6 (1)
4	sand at Ψm = -0.1 bars	70.8 ± 27	218 ± 45	2 (2)
5	Yolo at Ψm = -0.1 bars	7.0 ± 2.4	62 ± 14	2 (1)
6	sand at Ψm = -0.4 bars	(only reached 48-51% of total change)		2 (1)
7	Yolo at Ψm = -0.4 bars	(only reached 55-88% of total change)		2 (1)

B - dry sensor

#	time response in	63% of total change mean ± stand. dev. (hrs)	100% change mean ± stand. dev. (hrs)	No. of sensors
8	solution		206 ± 47	4 (1)
9	saturated sand		336 ± 38	2 (1)
10	saturated Yolo loam		352 ± 86	2 (1)
11	sand at Ψm = -0.4 bars	(only reached 12-56% of total change)		1 (2)
12	Yolo at Ψm = -0.4 bars	(only reached 28-68% of total change)		1 (2)

C - wet under vacuum sensor

#	time response in	63% of total change mean ± stand. dev. (hrs)	100% change mean ± stand. dev. (hrs)	sensors
13	solution	2.95 ± 1.08	359 ± 100	4 (1)

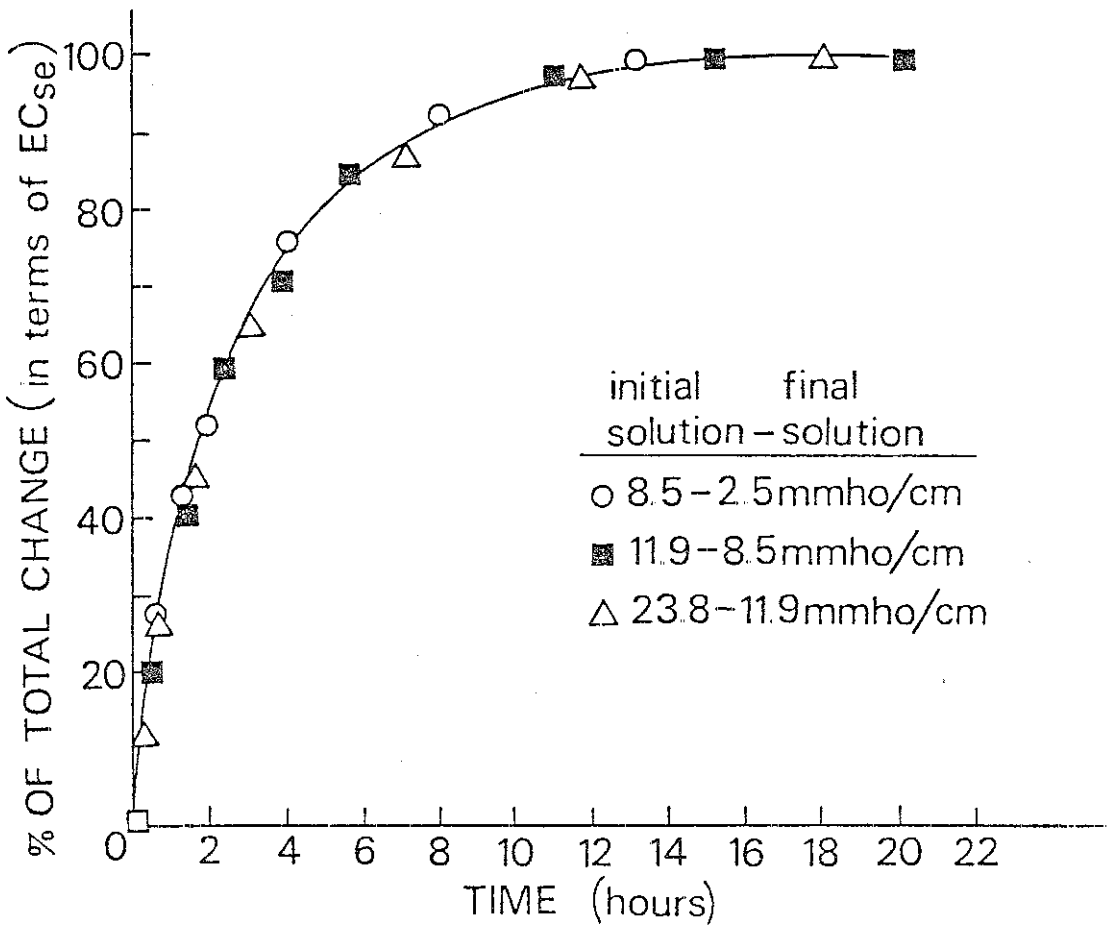

Figure 14. The time response in solution for sensors exhibiting normal behavior.

The response time of any sensor depends on the diffusion of solutes between the solution in the ceramic and the solution outside. Also, it depends on the geometry of the porous body, that is, on its thickness, uniform spacing and shape of electrodes, clay slips and firing procedures (Wesseling and Oster, 1973). Thus, the relatively high standard deviations of the means found in the experiments are not surprising. Even for the same sensor, response time among replications in unsaturated soils was substantially different, a fact that could be explained by the differences in contact between soil and sensors for different experiments.

For sensors of design similar to these, time response (63% change) in solution reported in the literature varied between one hour (Richard, 1966) and two hours (Wesseling and Oster, 1973), and total time response (100% change) was ten hours (Wesseling and Oster, 1973). The later authors also found that the sensor time response in a saturated sandy-loam soil was 50% of that obtained in bulk solution. From their analysis Wesseling and Oster (1973) concluded that time response in soil should remain constant over a wide range of water contents, but their work involved soil matric potentials no lower than -0.11 bars.

Table 7(A) shows that sensor time response is apparently influenced by the soil water content. Although the sand used in these experiments is probably not representative of a normal agricultural soil, experiment #6 shows that for Ψ_m = -0.4 bars, which corresponds to θ = 0.04 cm^3/cm^3 (Figure 15A), the sensor time response is practically infinite, an indication of the lack of film water contact between the soil and the sensor. Under these circumstances, the units will fail to

read the actual soil solution electrical conductivity. For Yolo loam, an agricultural soil extensively found in many areas of the county, sensor time response was also extremely slow for Ψ_m = -0.4 bars (experiment #7). For illustration, Figure 16A shows the extremes found in sensor time response for Yolo loam at Ψ_m = -0.4 bars (θ = 0.28 $cm^3 cm^{-3}$, Fig. 15B). At time zero, the sensor readings were of the order of 2 mmho cm^{-1}. The soil was equilibrated with a NaCl solution of EC = 6.6 mmho cm^{-1}. The decrease in sensor EC at time 30 hours is very significant as indicative of a partial desaturation of the sensor ceramic. In this case it seems that both matric potential sensitivity and lack of soil-sensor contact are responsible for the behavior of the sensor. As could be expected the slope of the time response curve for sand at Ψ_m = -0.4 bars (Figure 16B) was smaller than for the Yolo at the same matric potential. For sand, the matric potential effect was not as important as for Yolo loam because the low water content and subsequent lack of sand-sensor contact made the unit insensitive to it. This is reflected by the smaller desaturation of the sensor ceramic relative to that in Yolo loam.

In order to evaluate the influence of entrapped air on time response, experiment B - table 7(B) - was conducted. On the average, time response of a dry sensor (experiments 8, 9 and 10) increases about fourteen times in comparison with the saturated sensor (experiments 1, 2 and 3). The 63% change is not reported because of the unorthodox behavior of the units (Figure 17): apparently, the dissolution of salts precipitated in the conductance element is responsible for the sharp increase in EC during the first minutes. Thereafter, the relatively highly concentrated solution diffuses away from the sensor. The shape

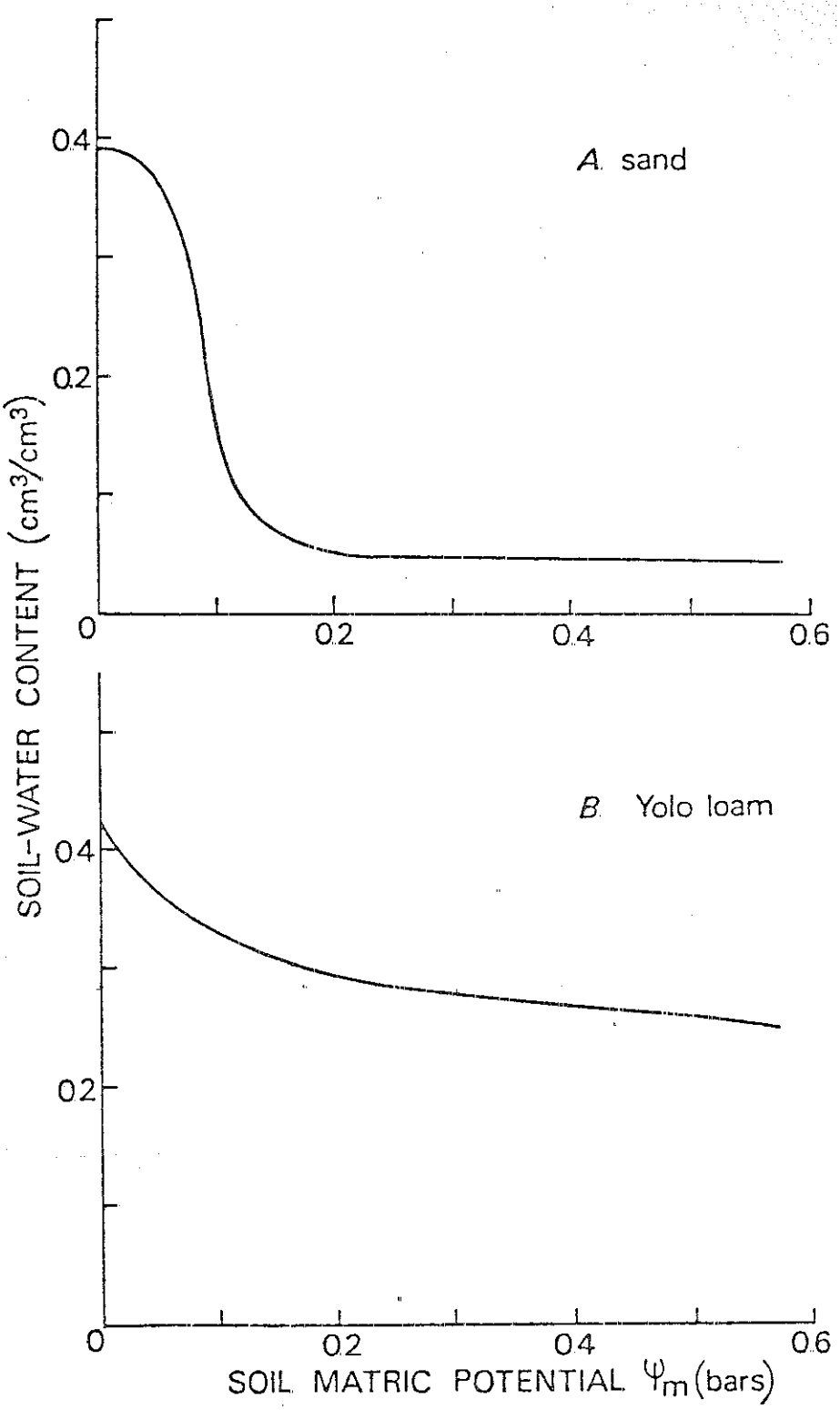

Figure 15. Soil-water characteristic curves for sand and Yolo loam soils.

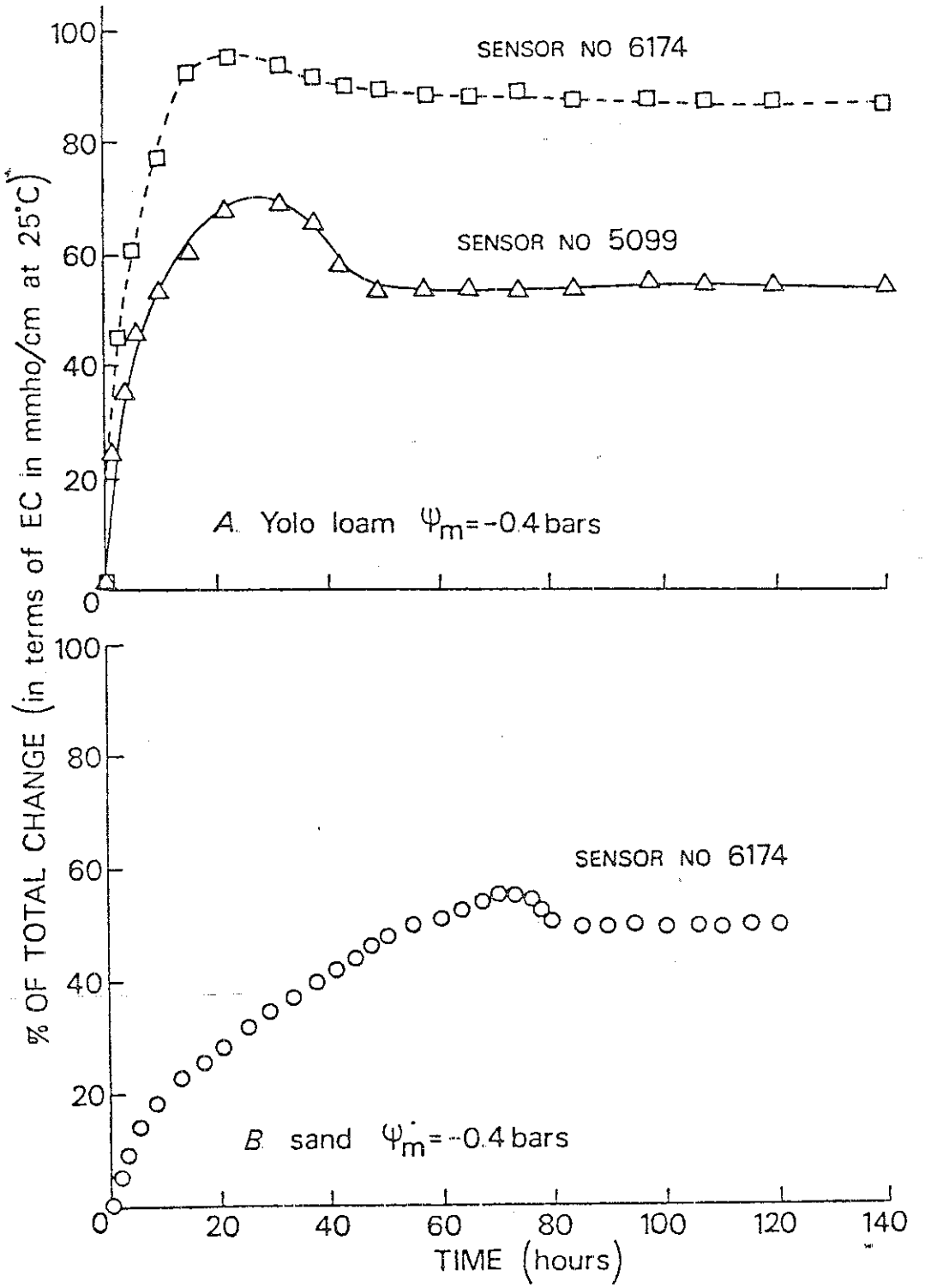

Figure 16. Sensor time response in partially saturated soils.
A. Yolo loam Ψm = -0.4 bars. B. Sand Ψm = -0.4 bars.

of the curve depends on the amount of salt precipitated in the sensor ceramic, on the concentration of the outside solution, and on the time needed for the empty pores to fill with solution. The last one will be mainly responsible for the shape of the curve after 20 hours. Therefore it is postulated that almost eight days are needed to resaturate a dry sensor. The same type of curves were found for the saturated soils (experiments 9 and 10), with the difference that fourteen days were needed for the sensors to resaturate and reach constant readings. As expected, the time needed for the dry ceramic to resaturate in partially-saturated soils (Table 7, experiments 11 and 12) is extremely long. The fact that in this case sensors are more sensitive to soil water content than to soil matric potential is demonstrated by comparing experiments 11 and 12. This leads to the conclusion that under these circumstances the main reason for the absence of a 100% response of the units is the lack of film water contact between the soil and sensor, as discussed above, rather than the geometry of the pores in the ceramic. It is therefore recommended that, before installation, sensors be kept in solution for at least 10 days, and if possible should be installed when the soil is at a relatively high water content.

Experiment C - table 7(C) - was conducted to confirm the existence of non-conductive pores. According to the limited results, the four sensors studied showed a long time response for the 100% change which suggested that all the units have non-conductive pores to some extent. However, if the geometry of these pores remains constant, the behavior of the sensors will not be greatly influenced by them. Figure 18 shows the shape of the time response curves for three of the sensors studied.

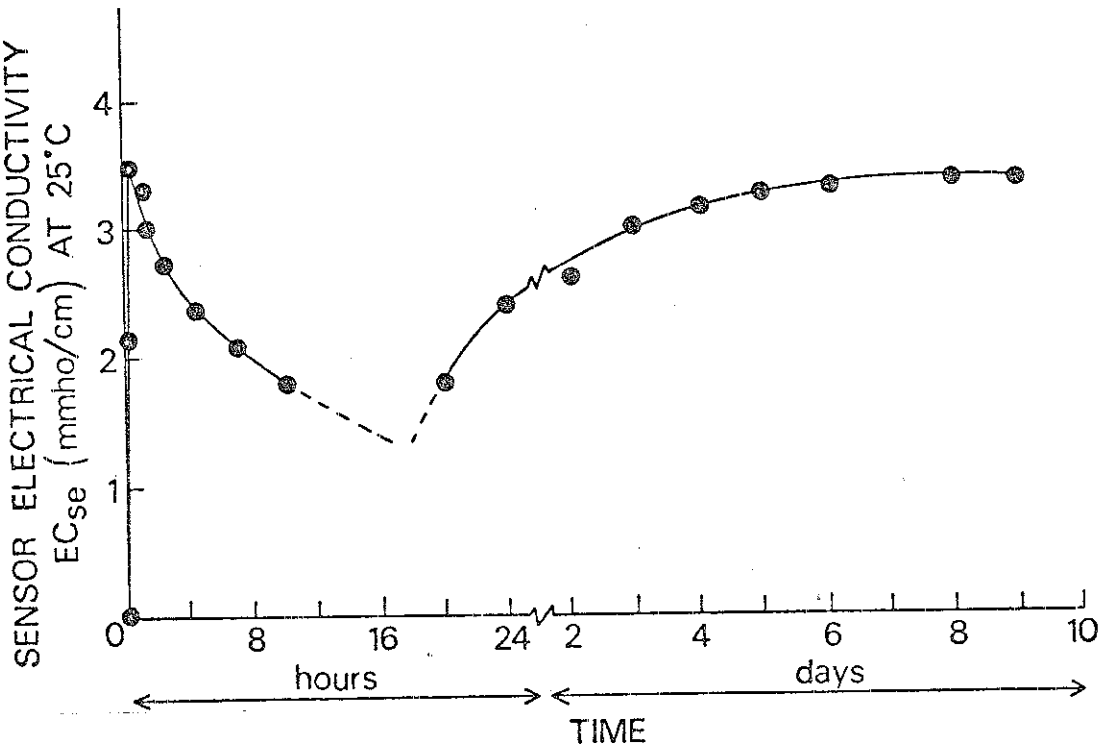

Figure 17. Time response of a dry sensor in solution.

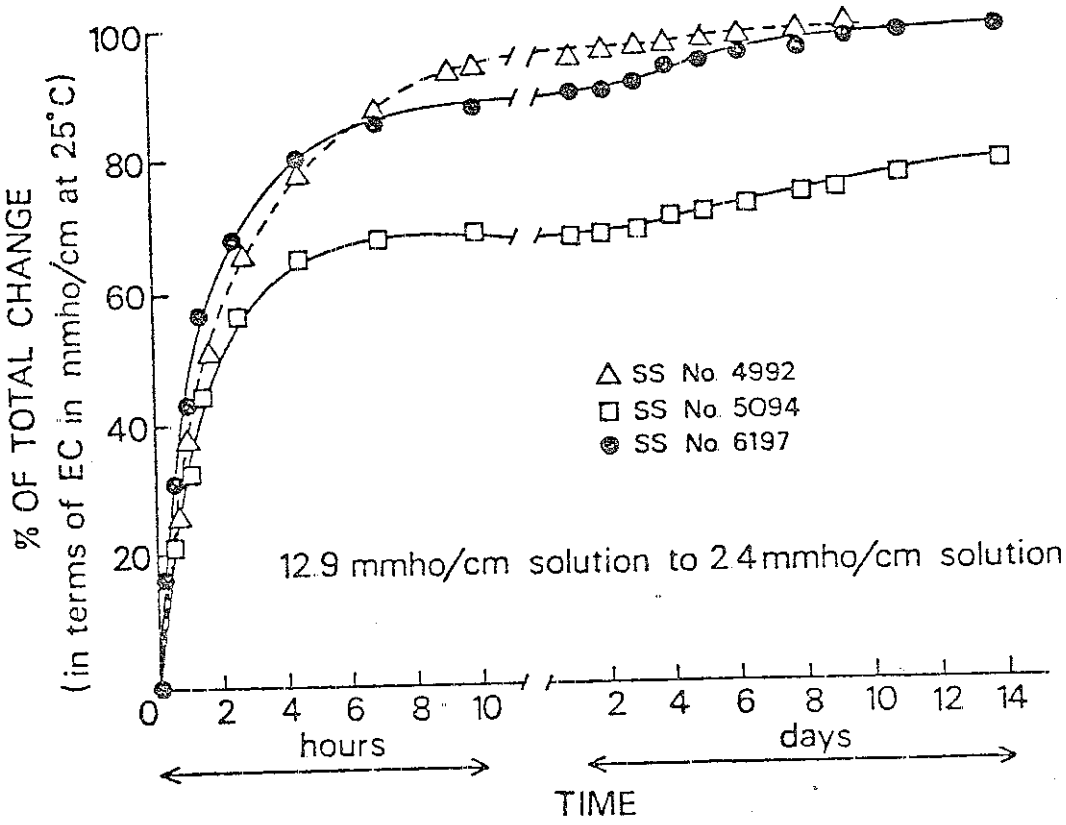

Figure 18. Time response in solution of sensors wet under vacuum.

The results for the sensor No. 6197 confirms the presence of stagnant pores in this unit (see hysteresis of calibration, p. 42), and indicates its lack of reliability. The application of this analysis to all sensors seems to be an adequate procedure to identify defective units.

In order to evaluate the reliability of the results obtained and relate them to a more realistic situation, the experiment described on p. 45 (see also Figure 13) was undertaken. Figure 19 shows the general sequence of changes in ECse (sensor electrical conductivity) and ECsp (electrical conductivity of the solution extracted by suction probe) due to changes in imposed solution concentrations for four porous media: cationic resin, Yolo loam, sand:kaolinite (2:1 by weight) and sand. Each triangle in the figure is an average of four salinity sensors. In order to account for a possible change in calibration, the results obtained were normalized in terms of per cent change of response. This was necessary because the experiment was done in mid-1976 and corrections were not made for a shift in calibration which may be particularly important at higher concentrations. Table 8 shows the time response (for a 63% change in ECse and ECsp) for the four porous media studied during the first 22 days of the experiment.

Figure 19 shows that data obtained by sensor measurements when the salinity changes occur over more than four days are reliable for all the porous media examined. However, when changes occur over less than four days (days 8 to 11 in the experiment) the sensors in the Yolo loam, and particularly in the sand-kaolinite column, were not able to reach the equilibrium concentration given by the solution extracted by the suction probe. This is also reflected in Figure 20, which shows the

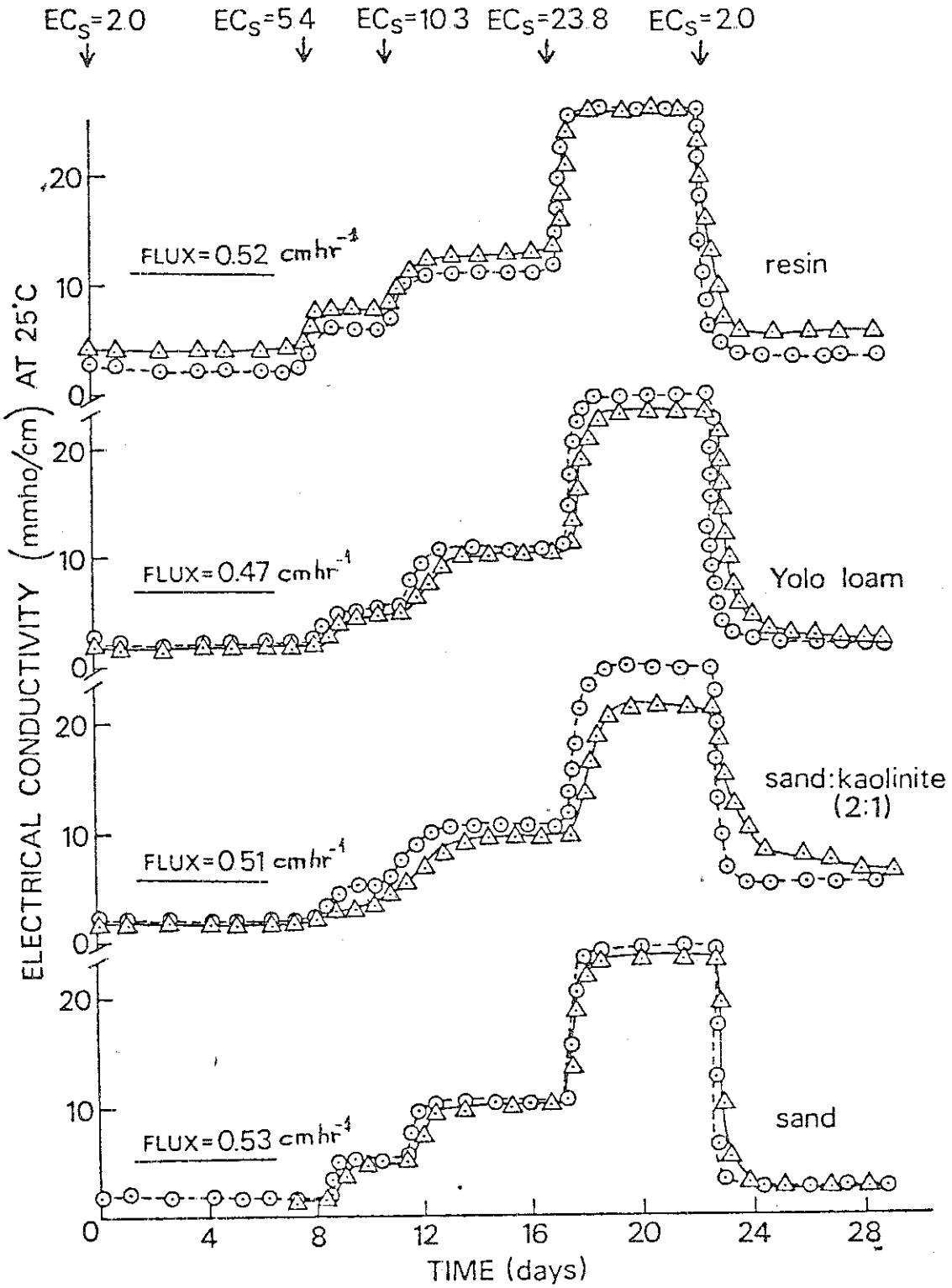

Figure 19. Response of salinity sensors (Δ) and suction probes (0) to solutions of various concentrations in four different porous media.

Table 8. Average time responses of sensors and suction probes in four porous media.

Porous Media	Time Response (hours) for 63% of total change				
	Suction Probe (SP) mean ± st. dev.	Salinity Sensor (SS) mean ± st. dev.	[SS-SP] mean	Number of SP samples	Number of SS readings
Resin	1.0 ± 0.4	2.8 ± 0.9	1.8	31	4x31
Yolo Loam	7.5 ± 0.8	12.0 ± 3.0	4.5	32	4x32
Sand:Kaolinite (2:1)	2.7 ± 1.0	17.3 ± 12.0	14.8	30	4x30
Sand	1.2 ± 0.1	4.6 ± 0.4	3.4	30	4x30

response of the sensors relative to the suction probes (ECsp/ECse).

From Figures 19 and 20 a clear distinction can be made between the resin and the other porous media. The sensor electrical conductivity (ECse) in the resin is always higher than the electrical conductivity of the solution extracted by suction probe (ECsp) while the opposite is true for the other three columns during the first 22 days of the experiment. This response might result from the high surface charge density of the resin (CEC = 10.2 meq gm^{-1}). The resin creates a large negative adsorption or salt exclusion in the liquid-solid interface with a resulting increase in the concentration of the soil solution with which the sensor is in equilibrium. As a result of the compression of the diffuse double layer, the salt exclusion effect decreases as the concentration of the imposed solution increases (Bower and Goertzen, 1955; Bolt and Bruggenwert, 1976) which is reflected in Figures 19 and 20. Further discussion on the effect of negative adsorption on sensor readings is given in Part VII (sensor sensitivity to negative adsorption).

The effect of the differences in pore size distribution of porous media on the behavior of sensors and suction probes is reflected in Table 8. If we assume that the solution in the sensor ceramic and the solution extracted by suction probes are similar at equilibrium, the differences in time response between the sensors and the suction probes (Table 8, fourth column) will be an indication of the time lag of sensors. Therefore, the values obtained should be similar to those in Table 7(A) (experiments 2 and 3). Thus, any value far apart from about 3.5 hours, (time response for sensors in saturated porous media), will be an indication of the inadequacy of the assumption, and will represent

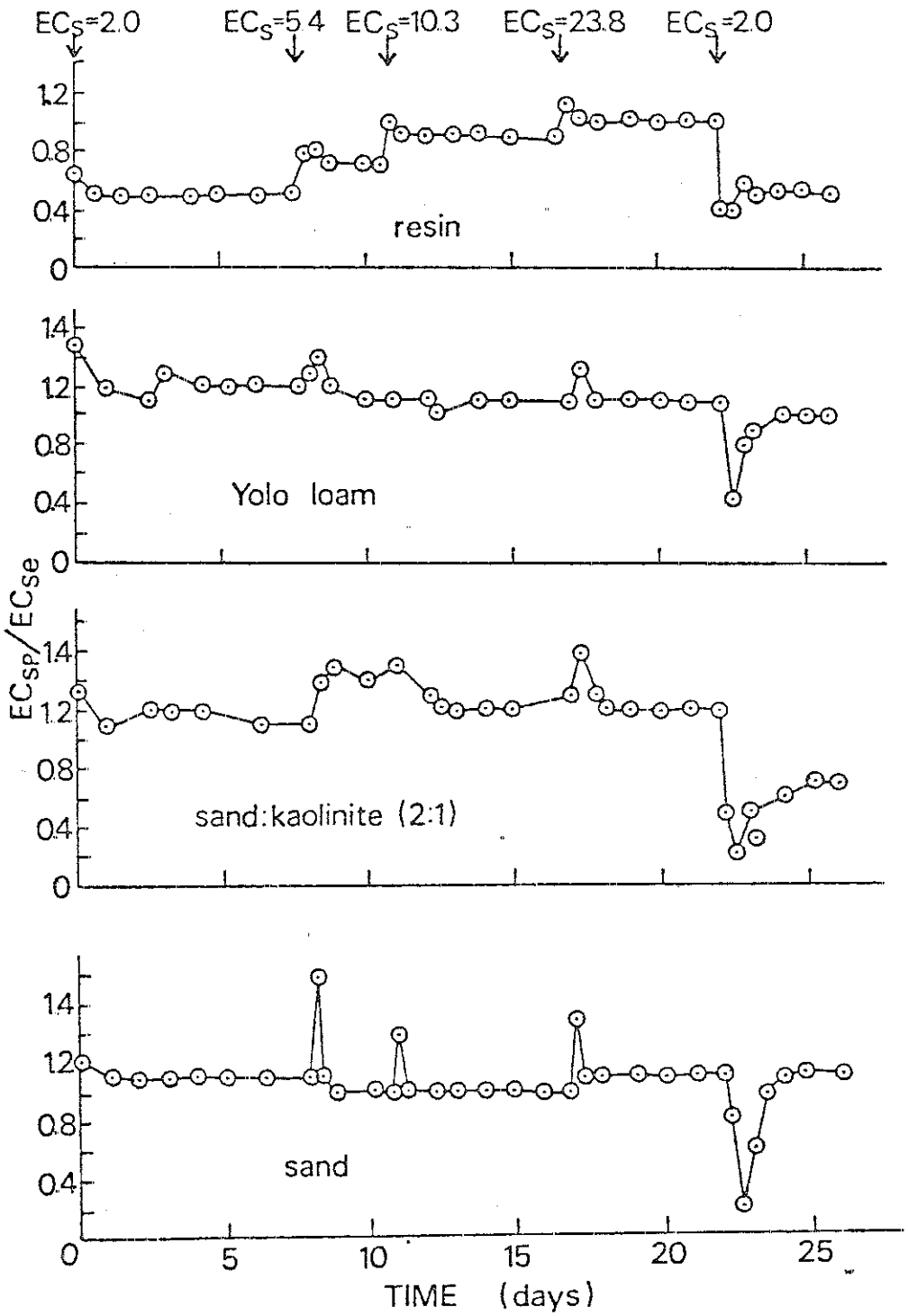

Figure 20. Response of the sensors relative to the solution extracted by suction probes (ECsp/ECse) to solutions of various concentrations in four porous media.

real differences in electrical conductivities of the soil solutions encountered. As we might expect, this is clearly reflected in the sand-kaolinite column due to the fact that only very large and very small particle sizes (sand and kaolinite respectively) predominate in the system. Whereas the solution extracted by suction probe might be expected to reflect the characteristics of the solution in the larger pores (Miller et al., 1965), the sensor may reflect the contact with the entire range of soil pores at its interface and therefore reduce the effect of the lack of dynamic equilibrium between soil pores. The extremely high standard deviation for the sensors in this column could be a reflection of the lack of homogeneity of the porous media as well as real differences in solution concentrations due to the distribution of the sensors in the column (Figure 13).

On the other hand, sensors in the sand column gave values very close to 3.5 hours, due to its narrow particle size distribution and relatively inert surfaces.

PART IV. External current of sensors

A. Procedure

The sensors were checked for the external flow of current in the solution by transferring them from the conductive solution into the nonconductive air and recording the change in resistance and sensor temperature with time. Care was taken to remove the solution clinging to the sensor with absorbent tissue. To check the influence that solution evaporation from the porous ceramic could have on the sensor temperature and therefore on the sensor conductance, a set of sensors were covered with parafilm paper at some time after removal from the conductive solution and readings taken as before. The external current was checked for four different conductive solutions in the range from 24 mmhos cm^{-1} to 2.5 mmhos cm^{-1}, including a saturated gypsum solution.

B. Results and Discussion

Figure 21A shows the general trend of the change in the average sensor resistance with time (for ten sensors), after the units are removed from the solution into the air, and Figure 21B shows individual changes in resistance for two particular sensors at four different initial solution concentrations. If we take the maximum percent change in resistance before it starts to decrease as indicative of the external flow of current, it will be 7.4 ± 1.5% (Fig. 21A) with no significant differences among the different solution concentrations (Fig. 21B).

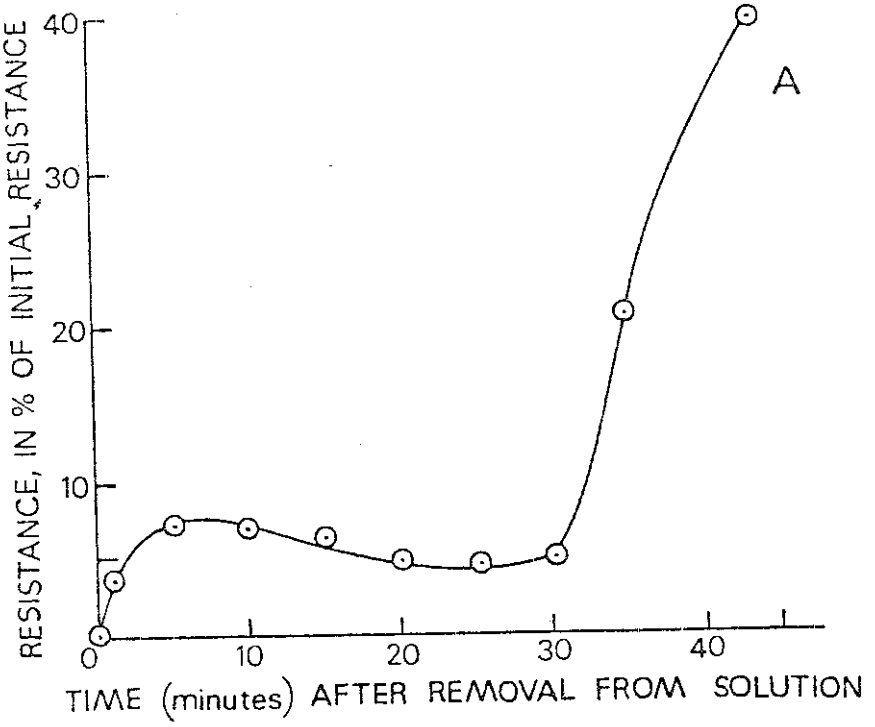

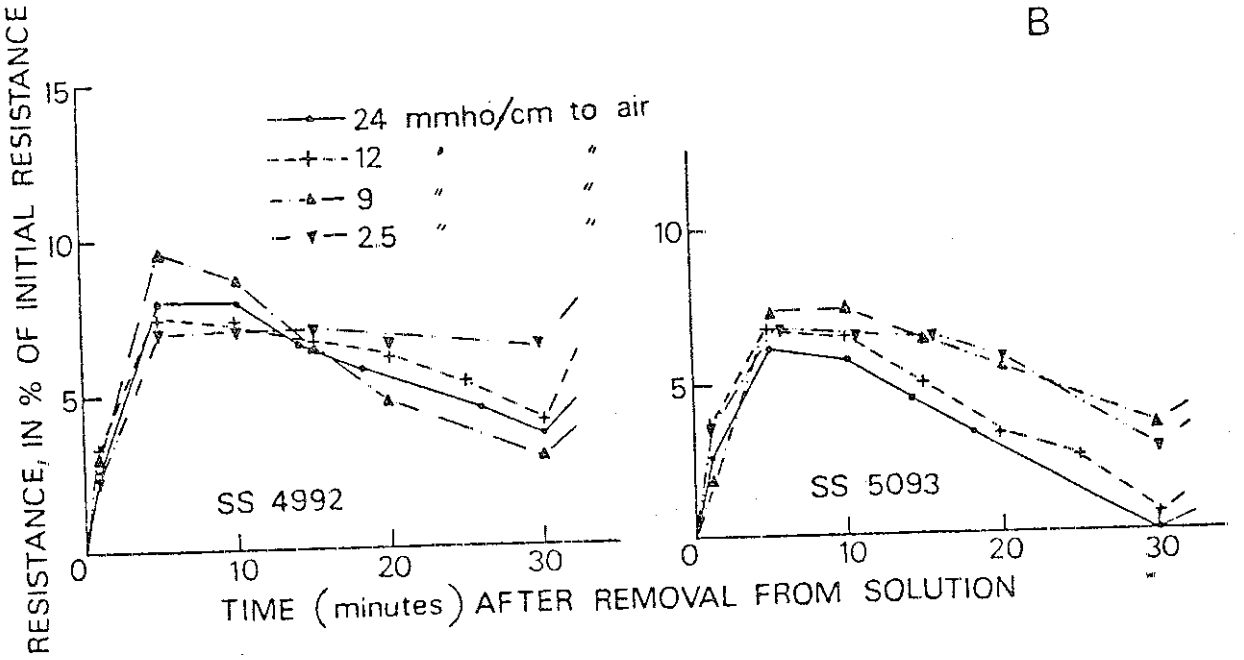

Figure 21. % change in sensor resistance with time when the sensors are moved from solution into air. A: average values for ten sensors and four solution concentrations. B: values for each solution concentration for two individual units.

However, although this estimate is close to that of Ingvalson et al. (1970) - 5% decrease in conductance -, the fact that from time 5 to time 30 there is a relative decrease in the resistance value leads to the conclusion that solution evaporation from the sensor surface was occurring, and therefore the values obtained were representatives of both external current and evaporation. The principal effects that the evaporation process will have on the units were thought to be: (i) A decrease in sensor temperature, which will tend to increase the sensor resistance, (ii) a decrease of the water content in the sensor ceramic, which will cause an increase in sensor resistance, and (iii) an increase in concentration of the solution remaining in the unit, which will tend to decrease the sensor resistance.

Point (i) was evaluated by measuring the thermistor resistance and converting it to degrees centigrade (Fig. 22). The sharp decrease in sensor temperature from 20 to 18.5°C in a period of 4 minutes, despite on the fact that the temperature gradient between the solution and the air was negligible, indicates the evaporation process. Taking into consideration this decrease in temperature, the estimated external flow of current for the example depicted will be less by one half. Also, figure 22 shows that when the sensor was covered with parafilm, the temperature increased, presumably due to the lack of evaporation, and it decreased again when the sensor was uncovered.

The effect of the increase in concentration of the solution in the sensor due to evaporation was evaluated by equilibrating two units with a saturated $CaSO_4 \cdot 2H_2O$ solution. A saturated gypsum solution will not concentrate but will precipitate. Figure 23 confirms that the resistance did not decrease as before, and the time for the abrupt

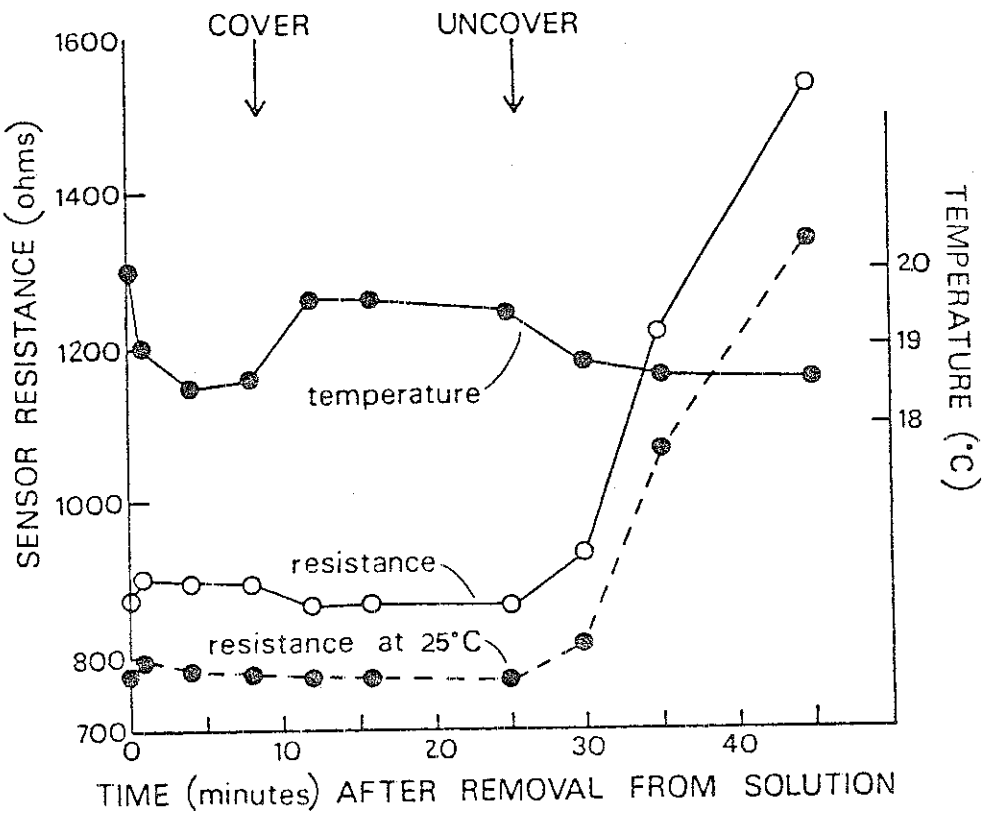

Figure 22. Change in sensor resistance with time when the sensors are moved from a 12 mmho cm^{-1} solution into air. At time = 8 min. the units were covered with parafilm.

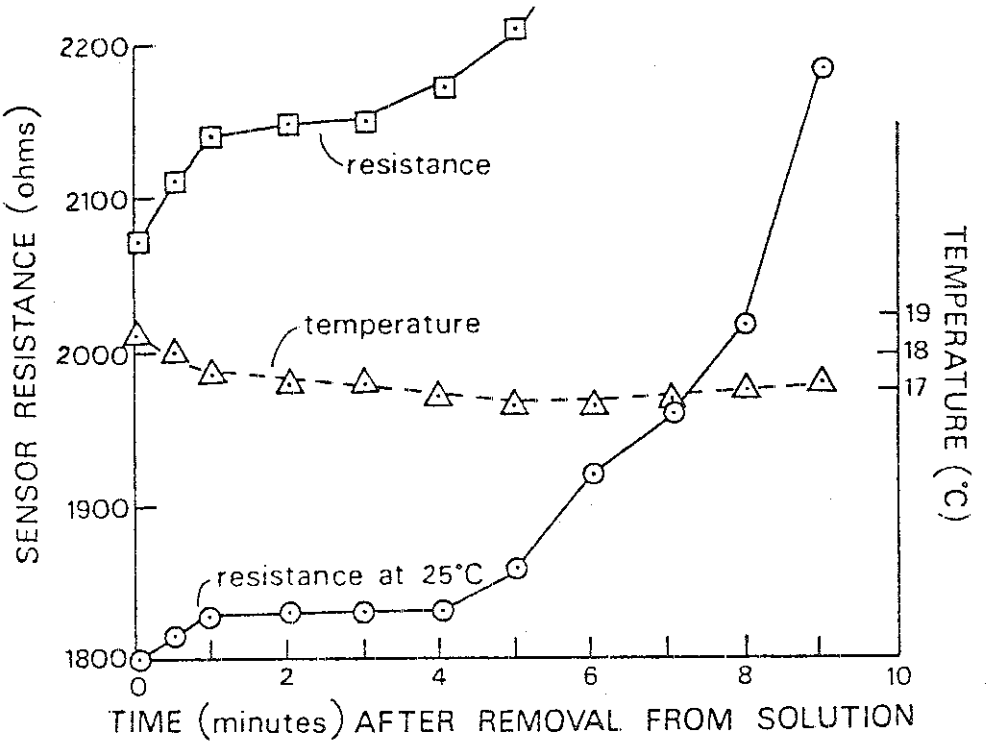

Figure 23. Change in sensor resistance with time when the sensors are moved from a saturated gypsum solution into air.

increase in resistance to occur decreased from 30 to about 4 minutes.

Finally the decrease of water content on the ceramic will be mainly responsible for the abrupt increase in the resistance at time 4 minutes.

To prevent the evaporation process which confounds the external flow value, an experiment was conducted in which ten units were covered with parafilm immediately after they were removed from the solution. Fig. 24 shows that the temperature did not decrease, but rather it tended toward room temperature (≃ 19.5°C) and that the resistance, after an increase of 0.7% (on the basis of the resistance at 25°C) remained constant with time. On the basis of these data, it was concluded that the external current of the salinity sensors was negligible (less than 1%).

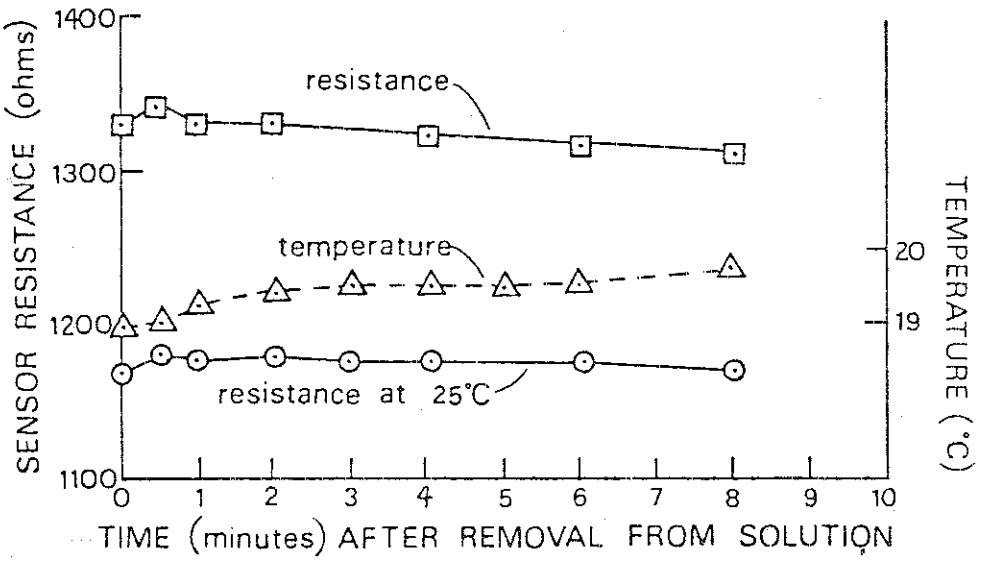

Figure 24. Change in sensor resistance with time when the sensors are moved from solution into air. At time = 0 min. the units were covered with parafilm to avoid evaporation.

PART V. Thermistor response and accuracy of sensors in measuring temperature

A. Procedure

A set of six sensors were placed in a constant temperature bath and readings of the thermistor resistance made at different times until equilibrium was achieved. The process was repeated for different bath temperatures in the range from 10 to 35°C. The time response of the thermistor element was checked by moving the sensors from a bath at 34.9°C to another at 23.0°C and measuring changes in thermistor resistance with time. The bath temperature was measured with a highly sensitive electronic thermometer (Omega Eng., Inc., Stamford, Conn.) and a copper-constantan thermocouple, type 3624T (accuracy = ± 0.5°C).

Once the thermistor resistance readings were recorded, the corresponding temperatures were determined as specified by the manufacturer.

B. Results and Discussion

The accuracy of the temperature (°C) measured by the thermistor in the sensors was evaluated. Table 9 shows the average values obtained from six sensors compared with the temperature of the bath. Figure 25 shows the time response needed to achieve the imposed temperature.

Time response (63% of the total change) was calculated to be 0.9 minutes, and the total time response 4 minutes, with an estimated accuracy of ± 0.3°C, which is better than the electronic thermometer

Table 9. Accuracy of temperature readings by the sensor thermistor. Values for average sensor temperature represent the mean ± standard deviation of six sensors.

Average bath temperature	10.3	18.4	22.7	26.5	29.6	34.9
Average sensor temperature	10.8 ± .21	18.5 ± .12	22.7 ± .14	26.3 ± .28	29.3 ± .08	34.4 ± .08
Difference ΔT (sensor-bath)	+0.5	+0.1	0.0	-0.2	-0.3	-0.5
% Error	4.9	.5	0	-.8	-1.0	-1.4

Avrg. STD DEV. = ± 0.15°C

Estimated Accuracy = ± 0.3°C

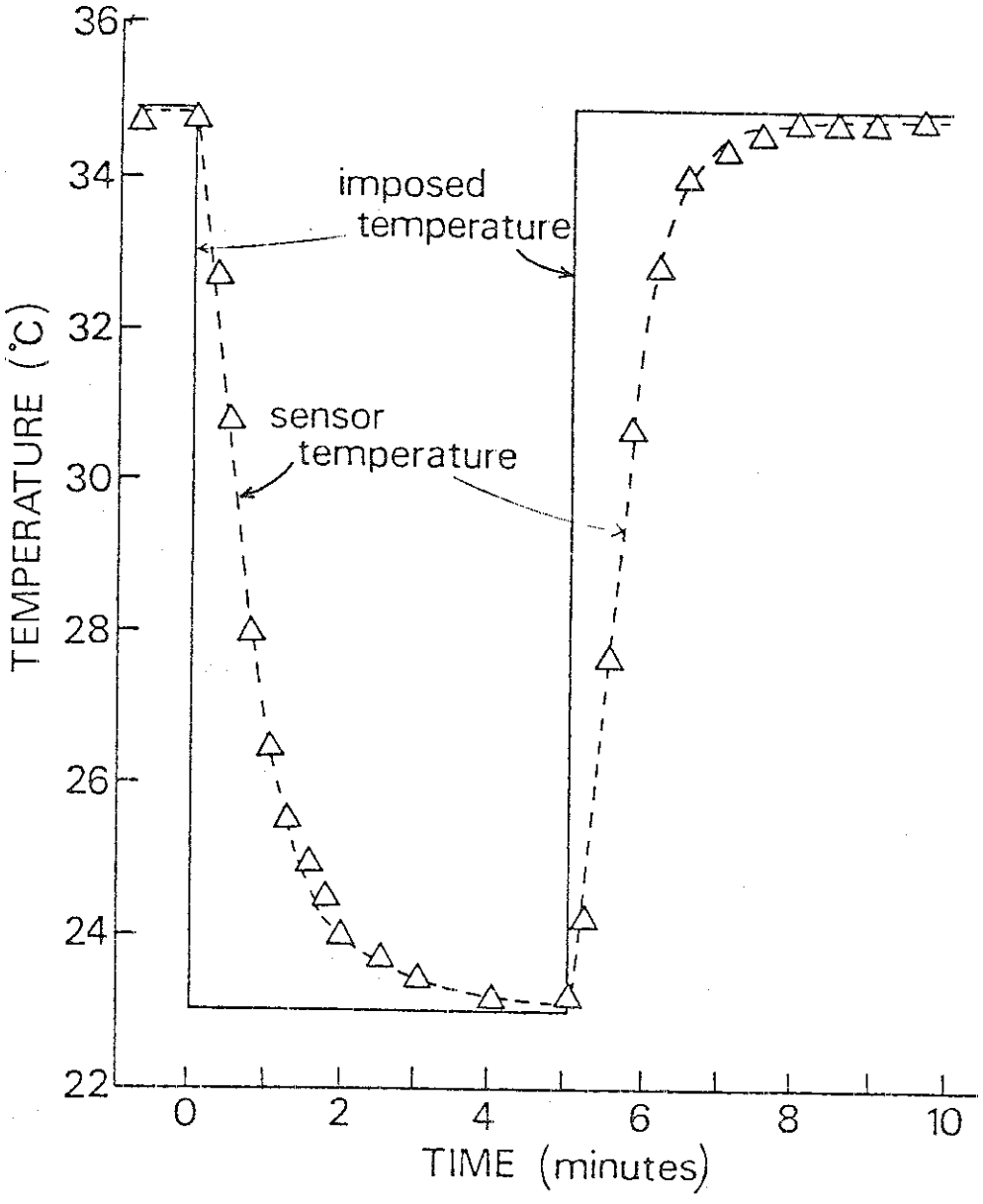

Figure 25. Time response of the sensor thermistor.

(± 0.5°C) used in the bath experiment. On the basis of these data, we concluded that the thermistor was accurate enough in the range from 10 to 35°C. Therefore, salinity sensors can be successfully used to measure temperature, an advantage that is frequently omitted in the literature.

PART VI. Sensor sensitivity to matric potential

A. Procedure

The salinity sensors were checked for sensitivity to decreasing soil matric potentials (Ψm) by two procedures:

a. For the range of relatively high Ψm (0 to -0.5 bars) the sensors were placed in a 600 ml buchner funnel (Pyrex No. 36060 F, Corning Inc., New York) filled with the previously prepared homoionic porous material. The fine porosity fritted disc was previously saturated with the same solution. The funnel was covered with parafilm paper to minimize evaporation (Figure 26). Initially, the sensors were allowed to reach equilibrium in the saturated soil. A definite Ψm corresponding to the vacuum applied was then imposed on the system, and sensor readings were taken daily until equilibrium was reached. The procedure was continued for decreasing Ψm until the air-entry value of the fritted disc was reached or until salinity sensor readings went off scale (EC < 1.5 mmhos cm^{-1}). Due to the relatively small distance between the sensors and the fritted glass, matric potential at the sensors was assumed to be the same as that at the plate.

After the EC of the sensors dropped an average of 50% from the initial value, the time that the partially desaturated sensor requires to resaturate and regain the initial EC at saturation was checked by resaturating the soil with the same solution as used previously.

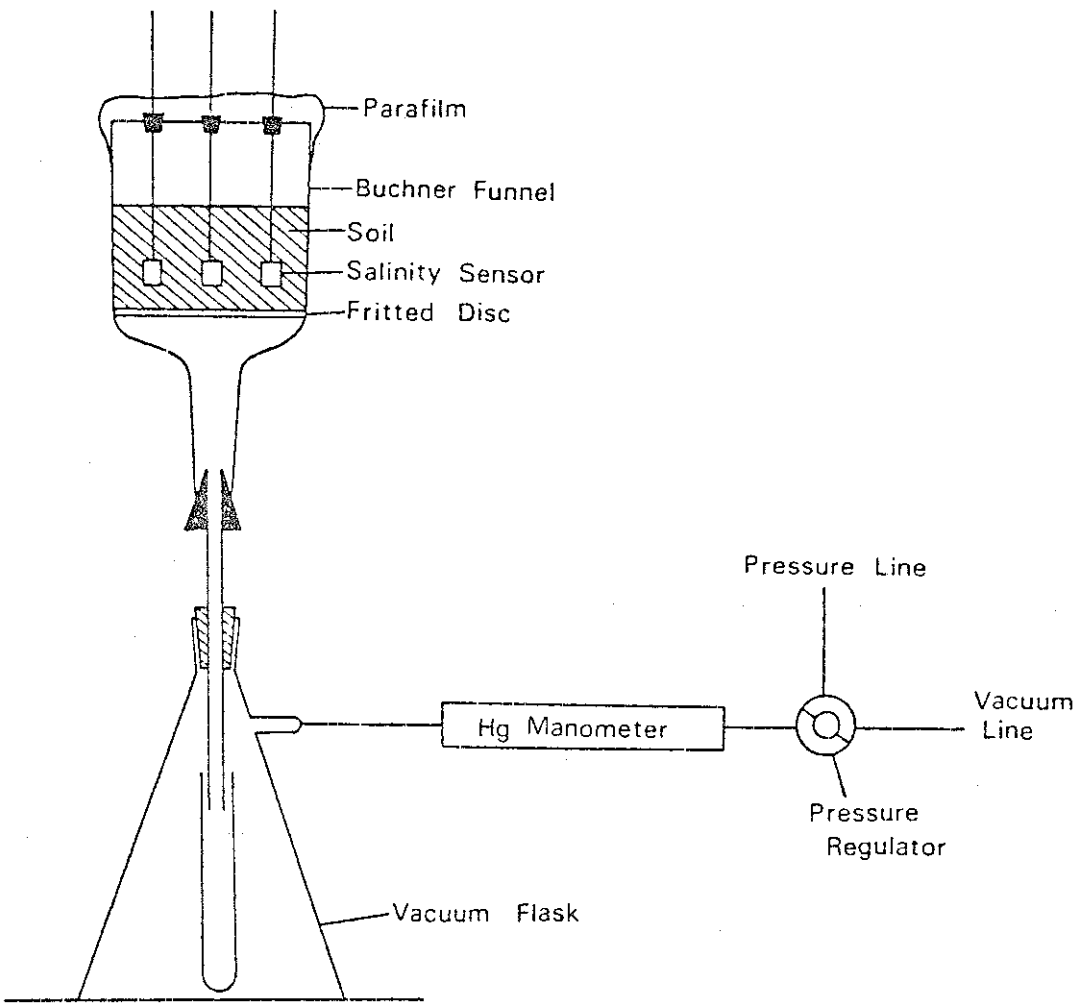

Figure 26. Experimental apparatus used to measure the sensor sensitivity to soil matric potential. Procedure a ("high" Ψm range).

b. For the range of "low" matric potentials (-1 to -15 bars) the sensors were attached to the conductors in the modified pressure plate apparatus (p. 16) and calibrated with NaCl solutions of known concentrations. The sensors were then installed in specially designed cylindrical containers placed on the saturated 15 bar ceramic plate and filled with the previously prepared homoionic soils. Thermocouple transducers were also installed at the same time (Figure 27).

After hydraulic and ionic equilibrium had been attained in the saturated soil, the sensor resistance was recorded and an increment of pressure was applied to force solution from the soil. When outflow had ceased and resistance readings remained constant for five days, a new increment was applied and the procedure continued for increasing applied pressures.

Due to the lack of accuracy and sensitivity of the thermocouple transducers the values obtained are not reported.

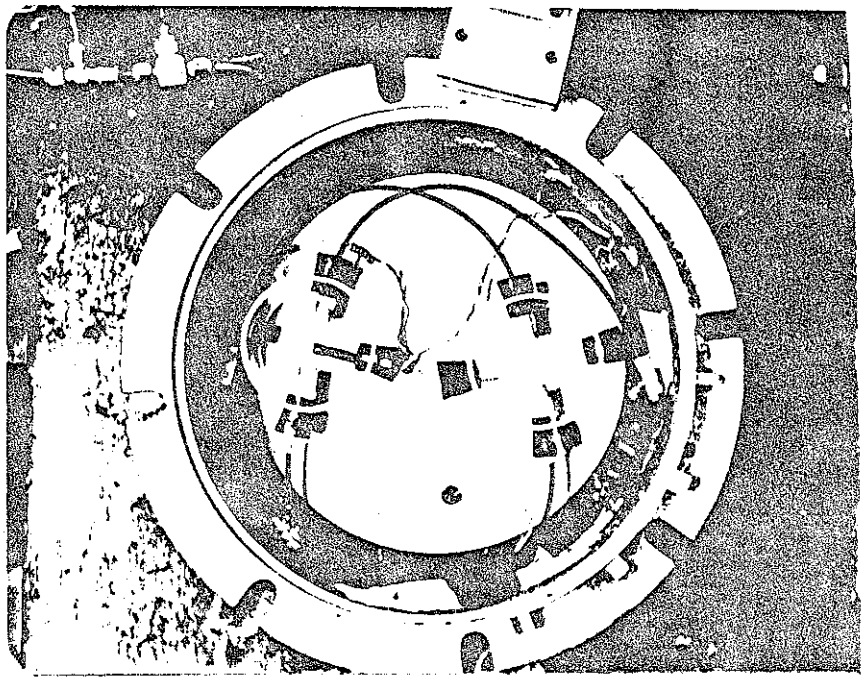

Figure 27. Experimental apparatus used to measure the sensor sensitivity to soil matric potential. Procedure b ("low" Ψ_m range).

B. Results and Discussion

Figure 28 summarizes the data obtained for all sensors and replications expressed in terms of the ratio ECi/ECs, where ECi is the sensor electrical conductivity at various Ψm and ECs is the sensor electrical conductivity at saturation. It is evident that this ratio ECi/ECs should be one or close to one at any soil matric potential if the reliability of the sensors is adequate. In Figure 28 the symbol | is used for the data obtained in procedure a (Figure 26) with parafilm cover. The symbol ▯ refers to the data obtained in the same set-up with the only difference being that the funnel was covered with wet cheese cloth and aluminum foil - besides the parafilm - trying to minimize evaporation. For relatively low Ψm (-0.7 to -4 bars) the modified pressure plate apparatus was used. Two symbols are given for this procedure in Figure 28 which refers to sensors equilibrated for 10 days in solution before being placed in the saturated soil (symbol |) and sensors wet under vacuum (symbol ▯).

The differences in behavior for equal Ψm of sensors in the sand and Yolo loam soils (procedure a, symbol |) suggest that the soil Ψm is not the only component to be considered for the interpretation of the results. Considering the possibility that some evaporation might be occurring, to which the sand will be much more sensitive (in terms of Ψm) then the Yolo loam, the funnels filled with sand were covered with wetted cheese cloth and aluminum foil to prevent it as much as possible. Figures 29 and 30 show the time sequence of the changes in sensor electrical conductivities with decreasing soil matric potentials for the sand and Yolo loam soils, respectively. At time 45 in Figure 29 the

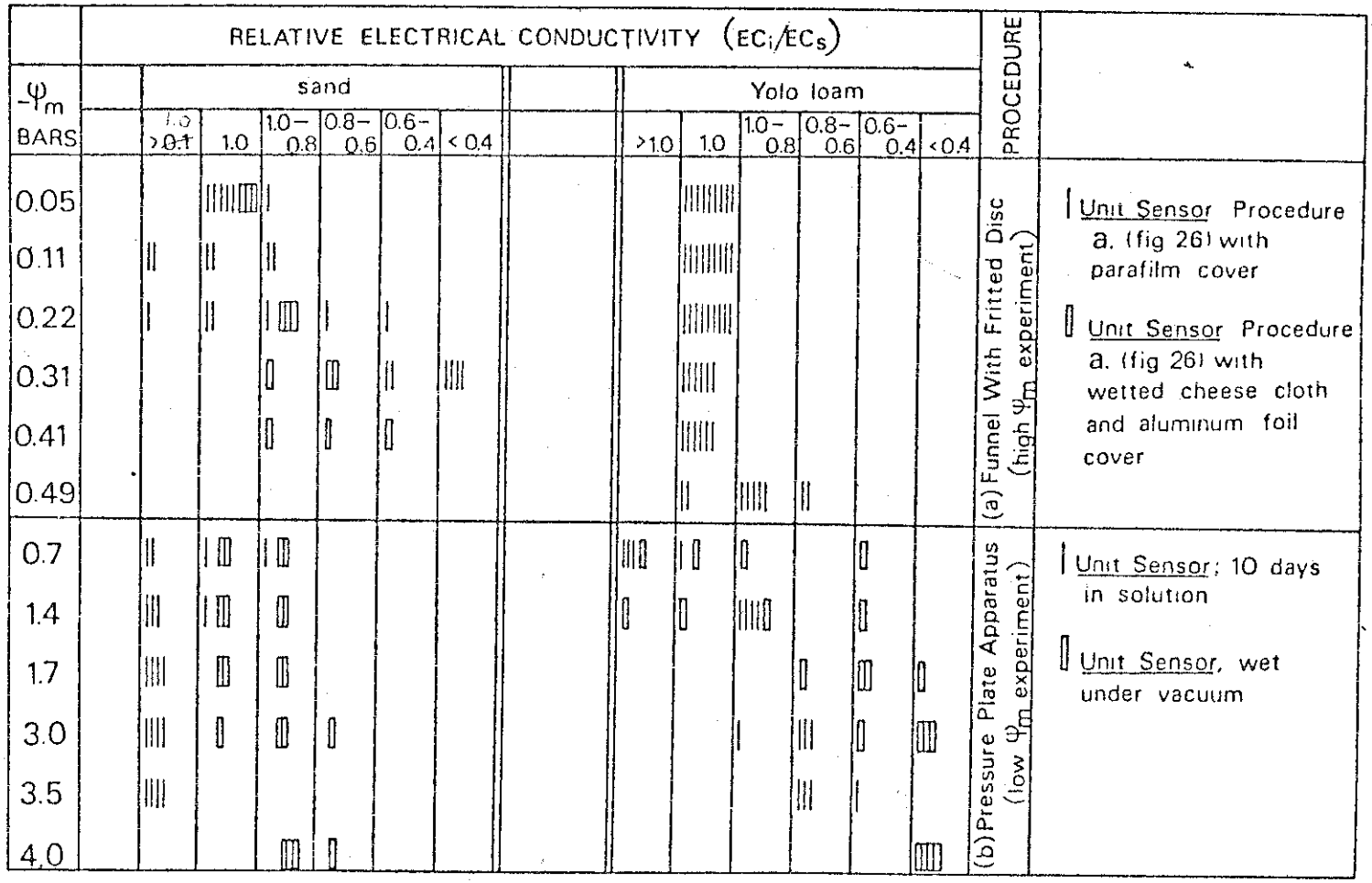

Figure 28. Relative EC of sensors (EC$_i$ sensor/EC$_s$ sensor of saturation) as a function of matric potential. Each symbol | and ▯ represents a single sensor and/or replication.

sand was resaturated with the same solution as used previously. Point 1 in Figure 30 indicates the point at which the air-entry value of the fritted disc was reached (day 48). Therefore the soil Ψm after this day was probably much lower than the imposed (-0.57 bars) due to drying of the soil by evaporation. The decreases in ECse after day 28 are therefore not computed in Figure 28.

Although the differences in sensor behavior for both soils decreased when the funnels filled with sand were covered with wetted cheese cloth and aluminum foil, it is apparent that whereas sensors in Yolo loam remain saturated (ECi/ECs = 1) for soil matric potentials of the order of -0.4 bars (Figure 30), the same sensors in sand showed a significant decrease in electrical conductivity readings for the same soil matric potential level (Figure 29). The reasons for these differences are not well understood, but it seems that the relatively lack of sand-sensor contact (due to the low soil water content at relatively high Ψm) together with solution evaporating from the sensor surface might be an important consideration. The fact that the time needed for the sensors to yield their EC values at saturation when the sand was resaturated (Figure 29, day 45) was more than 6 days suggest that desaturation of the sensor ceramic occurred because these large time responses are of the order of those found for a dry sensor (206 ± 47 hours).

The preliminary results obtained in the pressure plate apparatus were apparently opposite to those found in the fritted disc funnel; sensor electrical conductivities increased as the pressure applied increased in the sand, whereas for Yolo loam the opposite occurred. An explanation is that an increase in pressure causes a decrease in the

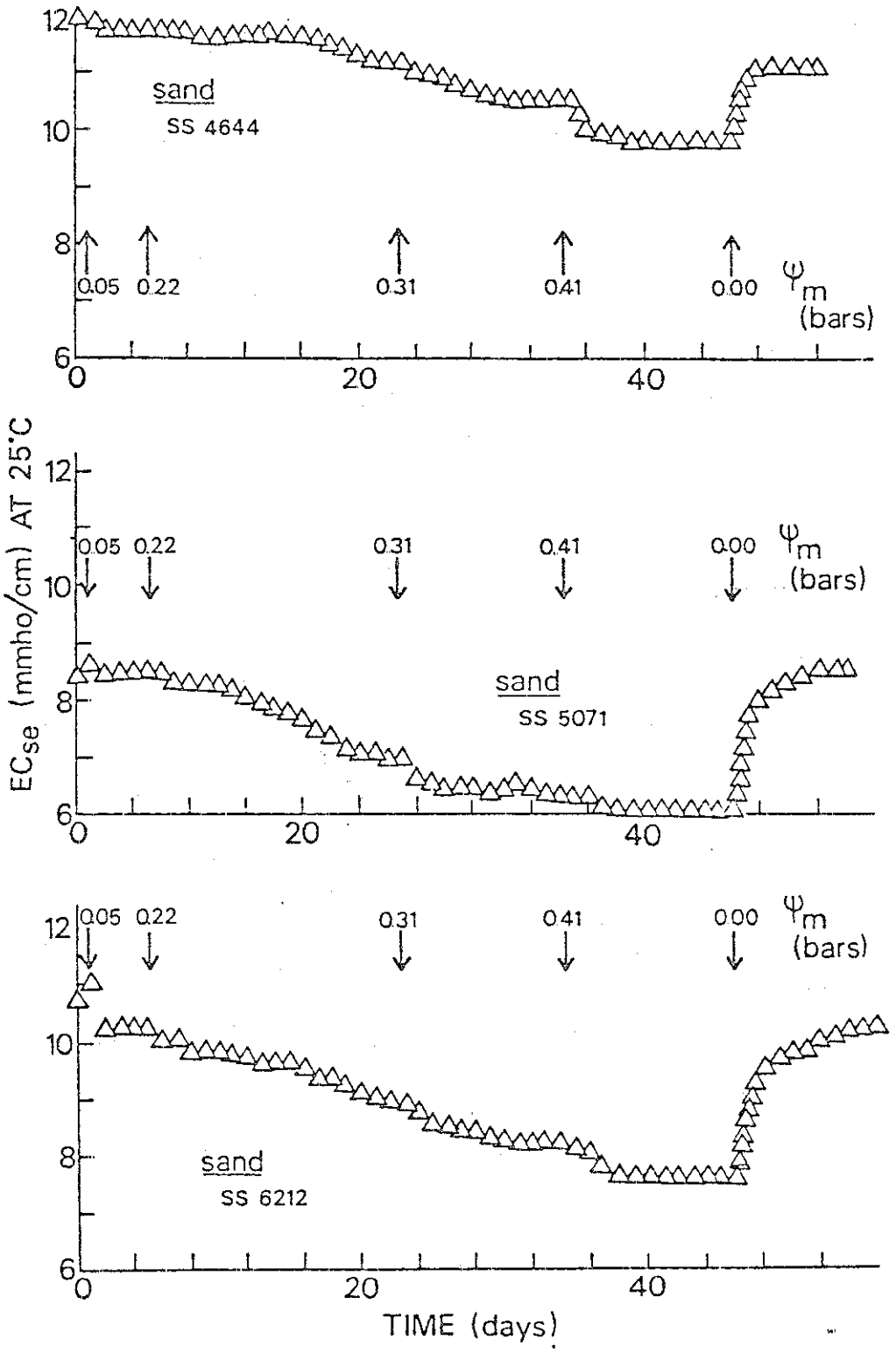

Figure 29. Time sequence of changes in sensor EC with decreasing sand Ψ_m. Arrows indicate the imposed soil matric potential. At day 46 the sand was resaturated (Ψ_m = 0.00).

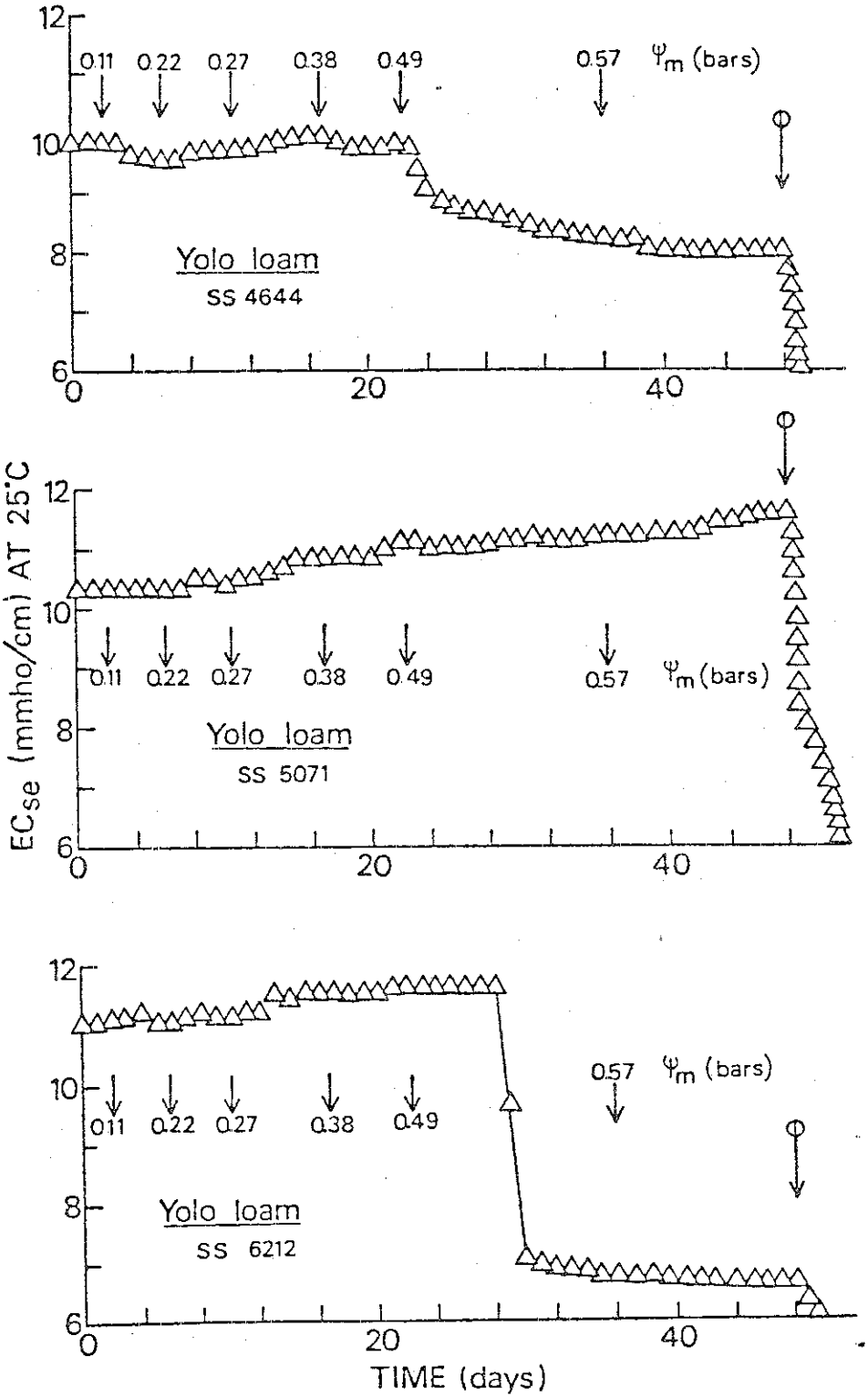

Figure 30. Time sequence of changes in sensor EC with decreasing Yolo loam Ψ_m. Arrows indicate the imposed soil matric potential. At day 48 the air-entry value of the fritted disc was reached.

volume of the air bubbles present in the sensor conductance element (which, in turn, tends to decrease the sensor resistance) and although the soil matric potential decreases to a value equal to the pressure applied, the lack of sand-sensor contact (due to the relatively low soil water content) makes the units insensitive to this decrease. On the other hand, sensors in contact with Yolo loam are sensitive to both phenomena, and the net result is a decrease in sensor electrical conductivity with increasing applied pressures. This hypothesis is confirmed by the behavior of the sensors when they were first wet under vacuum: (ECi/ECs) values for the units in contact with sand remain almost constant at values equal to one, whereas the sensor EC in Yolo loam decreased more drastically than before.

In conclusion, the behavior of salinity sensors in partially saturated soils is highly influenced by:

(i) Relatively low water contents ($\theta < 0.05$ cm^3cm^3) which result in lack of contact between the soil and the units and therefore in insensitivity to changes in soil solution EC.

(ii) Relatively low soil matric potentials ($\Psi m < -1$ bar) which result in desaturation of the sensor ceramic and therefore in lack of reliability to measure soil solution electrical conductivity.

PART VII. Sensor sensitivity to negative adsorption

A. Procedure

Systems of various montmorillonite:kaolinite ratios were prepared by mixing washed samples of pure bentonite and kaolinite minerals. These mixtures as well as a cationic resin sample were equilibrated and saturated with NaCl solutions of known concentrations, so that a total of 21 subsamples were prepared with a constant clay:solution ratio of 0.10:1 (gm:ml) (Table 10).

Salinity sensors were placed in mixtures of successively increasing montmorillonite:kaolinite ratios systems at the same salt content and finally in the cationic resin system. Sensor readings were recorded for each system after equilibrium was attained. These values were compared with the corresponding EC's of the solutions extracted by suction probes and with those of the NaCl solutions used in saturating the sub-samples. The same procedure was repeated in the reverse direction from low to high montmorillonite:kaolinite ratios.

Table 10. Subsamples of various montmorillonite:kaolinite ratios and various NaCl solution concentrations used to measure the sensor sensitivity to negative adsorption.

#	EC (mmho cm^{-1}) NaCl sln	% Montmor	% Kaol	#	EC (mmho cm^{-1}) NaCl sln	% Montmor	% Kaol
1	2.3	0	100	11	6.5	30	70
2	2.3	5	95	12	6.5	70	30
3	2.3	10	90	13	6.5	100	0
4	2.3	30	70	14	6.5	cationic resin	
5	2.3	70	30	15	12.9	0	100
6	2.3	100	0	16	12.9	5	95
7	2.3	cationic resin		17	12.9	10	90
8	6.5	0	100	18	12.9	30	70
9	6.5	5	95	19	12.9	70	30
10	6.5	10	90	20	12.9	100	0
				21	12.9	cationic resin	

B. Results and Discussion

Figure 31 shows the results obtained in this experiment. Part A refers to the EC values obtained in the solution extracted by suction probe, part B to the sensors placed in mixtures of successively increasing CEC's and part C to the sensors placed in mixtures of successively decreasing CEC's.

Only limited results can be given here due to the following difficulties encountered in the experiment:

(i) The clay: solution ratio of 0.1:1 (gm:ml) used was too high for the 100% Bentonite (CEC = 110 meq/100 gm) system and the resulting suspension was so dense that sensor readings were not consistent probably due to lack of contact between sensor and external solution. Also the time needed to extract enough solution from the 100% Bentonite system with the suction probe was more than five hours, giving rise to evaporation of the solution collected in the receiver and subsequent concentration. Thus, values for the 100% Bentonite system (CEC = 110 meq/100 gm) are not given.

(ii) The data obtained in the resin system were not comparable to the clay systems, probably due to differences in specific surfaces.

(iii) The time needed for the sensors to equilibrate with the different clay systems was extremely high, especially for the lower solution concentration and CEC's systems (up to 40 days). Due to limited time, we were not able to obtain replications.

(iv) Contamination of the solution extracted by Suction Probe was found to be important in some cases. Trying to minimize it, the probes were washed with about 100 ml of distilled water and let air-dry.

Successive 5 ml portions of the desired electrolyte were then extracted by applying suction to the probe immersed in the system of interest. By this procedure, in general the first 5 ml portion was found to be less concentrated than the subsequent portions, probably due to distilled water remaining in the pores of the probe. The values given in the figure correspond to the third portion of electrolyte extracted which in general was close to the second extracted portion.

With these limitations in mind, the results obtained (Fig. 31) clearly suggest the importance of negative adsorption on the sensor behavior. Negative adsorption of anions or salt exclusion (Reitemeier, 1946; Schofield, 1947; Babcock, 1963) results from a deficit in anion concentration close to the surface of soil particles caused by the negatively charged particle surfaces. This decrease in anion concentration results in salt exclusion near particle surfaces with a resulting increase in the concentration of the soil solution further from the surfaces. According to the double layer theory (Babcock, 1963) and experimentally confirmed (Bower and Goertzen, 1955; De Haan, 1965), salt exclusion increases with an increase in the specific surface of the soil and with a decrease in the electrolyte concentration. Consequently the concentration of the solution in the sensor ceramic which is in equilibrium with the soil solution would also be increased. The data shown in Figure 31 are in accordance with the above description.

A few interesting remarks can be made about the results:

(i) The slope of the curves for the sensors are larger than the corresponding slopes of the suction probes, except for the highest electrolyte concentration. This suggest that under our experimental conditions the solution extracted by suction probes is from a region

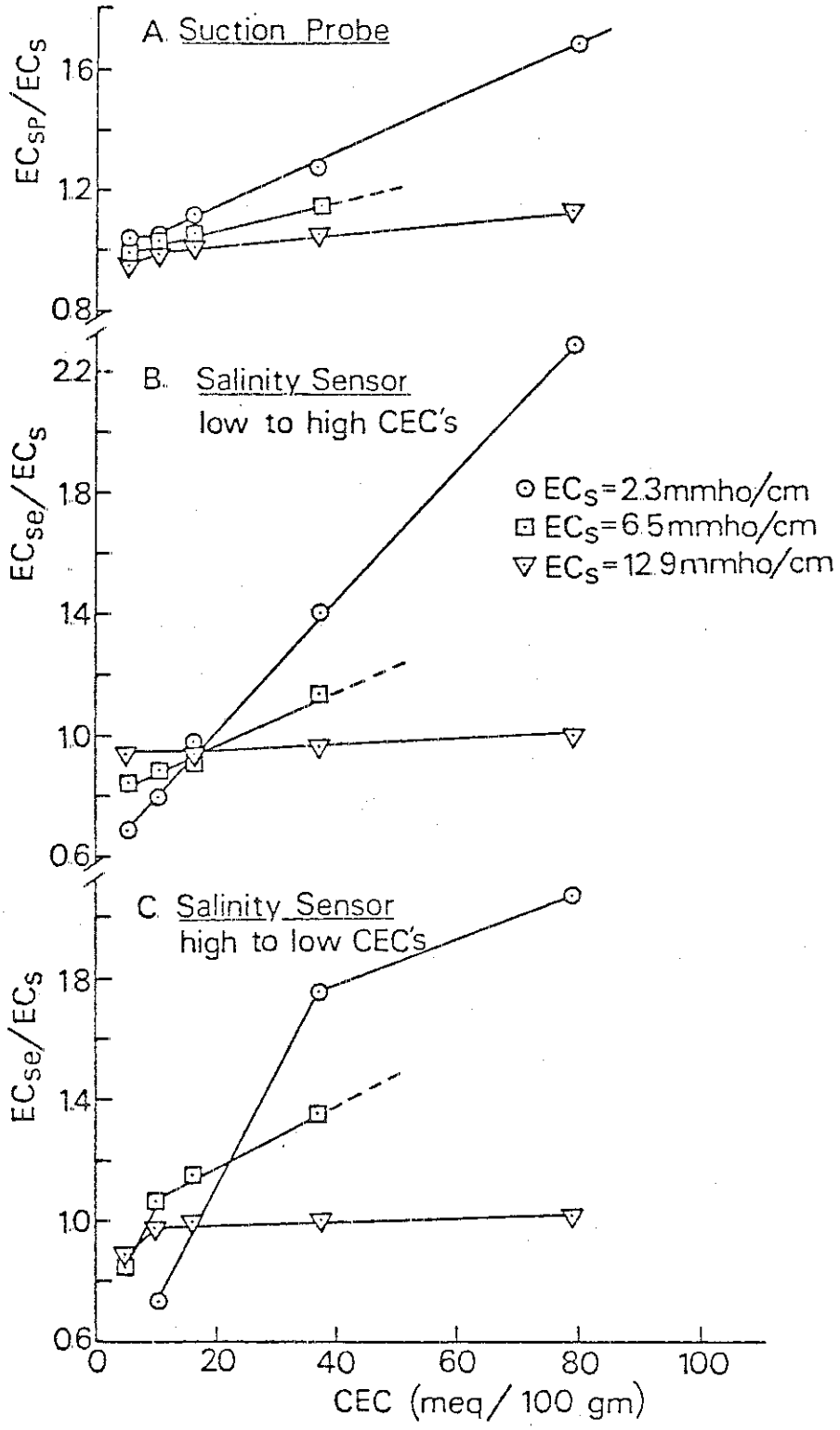

Figure 31. Relative EC of sensors for increasing montmorillonite: kaolinite ratios.

relatively closer to the clay surfaces - in other words, is relatively less concentrated - compared with the solution with which the sensors are in equilibrium or is from a region contained mainly in the larger pores. As could be expected the slopes are similar at the highest concentration level (ECs = 12.9 mmho cm^{-1}) for which the salt exclusion effect is of much less relative importance. The larger area of the suction probe compared with that of the sensor as well as the vacuum level applied for extracting the solution might be also of significance in trying to explain these differences.

(ii) The minor differences in behavior when the sensors were moved from the lower to the higher CEC systems (case B) or from the higher to the lower CEC systems (case C) may be important. It seems that the history of the sensor might be considered, but more work should be done to elucidate its significance.

(iii) The ratios ECse/Ecs are less than unity for the lower CEC systems. Although several reasons could contribute to this behavior, such as specific adsorption of the chloride ion on the exposed alumina of kaolinite surfaces (Bolland et al., 1976) or the presence of some water in the Kaolinite mineral, an important reason could be the salt exclusion effect of the sensor ceramic which will act as a salt sieve in the opposite direction to the salt exclusion of the clay systems mentioned above. At the lower CEC the relative importance of the salt sieving effect of the sensor ceramic will be increased, and therefore the concentration of the solution in the ceramic will decrease relative to that outside the sensor. This phenomenon seems to be of less significance for the suction probe as could be expected due to the relatively larger pore sizes of the ceramic in the probe compared with

those in the sensor. The conclusion is that the sensor ceramic is not as inert as might be thought, and that it shows surface properties which could be of significance under certain circumstances. This will have important implications in terms of interactions in the sensor ceramic-liquid interface and poses additional questions which should be elucidated for a better understanding of the reliability and limitations of soil salinity sensors.

SUMMARY AND CONCLUSIONS

Commercial salinity sensors were evaluated on the following aspects: (i) correlation between sensor electrical conductivity and solution extracted by suction probe, (ii) calibration of sensors, (iii) time response of sensors (defined as the time required for sensors to reach 63% (or 100% as indicated) of equilibrium response when moving the sensors from one concentration level to another), (iv) external current of sensors (flow of current outside the porous body of the units), (v) thermistor response and accuracy in measuring temperature, (vi) sensor sensitivity to decreasing soil matric potentials and (vii) sensor and suction probe sensitivity to negative adsorption or salt exclusion.

The results of this study suggest the following conclusions:

(i) The correlation of the results obtained between the sensors and suction probes is good except for those cases of porous media with a wide range of pore size distributions or systems of relatively high surface charge properties.

(ii) The presence of stagnant or non-conductive pores in the ceramic of some sensors is postulated and its negative effects on calibration, hysteresis and time response of sensors is discussed.

(iii) Only 23% of the sensors examined were considered to be stable over a period of fourteen months of operation. Of the unstable sensors, 93% showed a typical shift in calibration which leads to underestimates of the soil electrical conductivity, especially at higher concentrations. Precipitation of salts within the ceramic is thought to be an important reason for the instability of the salinity sensors.

(iv) The estimated accuracy of EC measured by the sensors after more than one year of operation is ± 0.8 mmho cm^{-1} for the stable and corrected unstable sensors and ± 2 mmho cm^{-1} for the non-corrected, unstable sensors.

(v) Time response of sensors in solution and saturated porous media is adequate for most practical situations, but it is extremely long for partially saturated soils (Ψm = -0.4 bars). Lack of contact between soil and sensor and discontinuities in the pore geometry of the units are thought to be responsible for such long time responses.

(vi) The external current of sensors is negligible (less than 1% of the resistance).

(vii) The time response (0.9 minutes for a 63% of total change) and accuracy (±0.3°C) of the thermistor element makes the sensor a practical tool for monitoring temperature.

(viii) The behavior of sensors in partially saturated soils is highly influenced by the soil water content (θ < 0.05 cm^3cm^3) which results in lack of contact between sensor and soil solution and by the soil matric potential (Ψm < -1 bar) which results in desaturation of the sensor ceramic.

(ix) The effect of negative adsorption in increasing sensor EC values is demonstrated. The salt sieving of the sensor ceramic clay is suggested as a possible explanation of the results obtained, but the limited data do not allow any definite conclusion on this point.

BIBLIOGRAPHY

Babcock, K. L. 1963. Theory of the chemical properties of soil colloidal systems of equilibrium. Hilgardia 34: 417-542.

Bower, C. A. and J. O. Goertzen. 1955. Negative adsorption of salts by soils. Soil Sci. Soc. Am. Proc., 19: 147-151.

Bolt, G. H. and M. G. M. Bruggenwert. 1976. Soil Chemistry A. Basic Elements. Elsevier Pub. Co., Inc., New York. 281 p.

Bolland, M. D. A., A. M. Posner and J. P. Quirk. 1976. Surface charge on Kaolinites in aqueous suspension. Australian Journal of Soil Res., 14(2): 197-216.

Briggs, L. J. and A. G. McCall. 1904. An artificial root for inducing capillary movement of soil moisture. Science, Vol. XX, No. 513: 566-569.

De Haan, F. A. M. 1965. Determination of the surface area of soils on the basis of anion exclusion measurements. Soil Sci., 99: 379-386.

Enfield, C. G. and D. D. Evans. 1969. Conductivity instrumentation for in-situ measurement of soil salinity. Soil Sci. Soc. Amer. Proc., 33: 787-789.

Hansen, E. A. and A. R. Harris. 1975. Validity of soil-water samples collected with porous ceramic cups. Soil Sci. Soc. Am. Proc. 39: 528-536.

Harris, A. R. and E. A. Hansen. 1975. A new ceramic cup soil-water sampler. Soil Sci. Soc. Am. Proc., 39: 157-158.

Ingvalson, R. D., J. D. Oster, S. L. Rawlins, and G. J. Hoffman. 1970. Measurement of water potential and osmotic potential in soil with a combined thermocouple psychrometer and salinity sensor. Soil Sci. Soc. Am. Proc., 34: 570-574.

Jackson, M. L. 1974. Soil Chemical Analysis. Advanced course. M. L. Jackson, Madison 6, Wisconsin. 895 p.

Kapp, L. C. 1937. Extracting a submerged soil solution. Arkansas Agric. Exp. Sta. Bull. 351, p. 28.

Kemper, W. D. 1959. Estimation of osmotic stress in soil water from the electrical resistance of finely porous ceramic units. Soil Sci. 87: 345-349.

Miller, R. J., J. W. Biggar and D. R. Nielsen. 1965. Chloride displacement in Panoche clay loam in relation to water movement and distribution. Water Res. Res. 1: 63-73.

Oster, J. D. and R. D. Ingvalson. 1967. In-situ measurement of soil salinity with a sensor. Soil Sci. Soc. Am. Proc., 31: 572-574.

Oster, J. D., S. L. Rawlins and R. D. Ingvalson. 1969. Independent measurement of matric and osmotic potential of soil water. Soil Sci. Soc. Am. Proc., 33: 188-192.

Oster, J. D. and L. S. Willardson. 1971. Reliability of salinity sensors for the management of soil salinity. Agronomy Journal 63: 695-698.

Oster, J. D. and B. L. McNeal. 1971. Computation of soil solution composition variation with water content for desaturated soils. Soil Sci. Soc. Am. Proc., 35: 436-442.

Parker, F. W. 1925. The absorption of phosphates by Pasteur-Chamberland filters. Soil Sci., 20: 149-158.

Reeve, R. C. and E. J. Doering. 1965. Sampling the soil solution for salinity appraisal. Soil Sci., 99: 339-344.

Reicosky, Donald C., R. J. Millington, and D. B. Peters. 1970. A salt sensor for use in saturated and unsaturated soils. Soil Sci. Soc. Am. Proc., 34: 214-217.

Reitemeier, R. F. 1946. Effect of moisture content on the dissolved and exchangeable ions of soils of arid regions. Soil Sci. 61: 195-215.

Rhoades, J. D. 1972. Quality of water for irrigation. Soil Sci. 113: 277-283.

Richards, L. A. 1966. A soil salinity sensor of improved design. Soil Sci. Soc. Am. Proc., 30: 333-337.

Schofield, R. K. 1947. Calculation of surface areas from measurements of negative adsorption. Nature 160: 408-410.

Todd, R. M. and W. D. Kemper. 1972. Salt dispersion coefficients near an evaporating surface. Soil Sci. Soc. Am. Proc., 36: 539-543.

US Salinity Laboratory Staff. 1954. Diagnosis and improvement of saline and alkali soils. US Dep. Agr. Handbook 60. 160 p.

Wesseling, J. and J. D. Oster. 1973. Response of salinity sensors to rapidly changing salinity. Soil Sci. Soc. Am. Proc., 37: 553-557.

Wolff, R. G. 1967. Weathering woodstock granite near Baltimore, Maryland. Amer. J. Sci., 265: 106-117.

APPENDIX

Regression analysis performed on each of the sensors for
libration 1975a (manufacturer's calibration) and calibration 1976.

LEGEND

Regression Line Cse = A + B ECs,

ere: Cse = sensor conductance in mmhos at 25°C

A = intercept (mmhos)

B = slope (cm)

ECs = electrical conductivity of the solution in mmho cm^{-1} at 25°C

S_A = standard deviation of A

S_B = standard deviation of B

r = correlation coefficient

Salinity sensor cat. No.	Calibration 1975a					Calibration 1976				
	Cse = A + B ECs					Cse = A + B ECs				
	A	B	S_A	S_B	r	A	B	S_A	S_B	r
4601	0.257	0.0769	0.0207	0.0022	0.9984	0.244	0.0738	0.0396	0.0028	0.9971
4604	0.243	0.0713	0.0194	0.0020	0.9984	0.262	0.0633	0.0337	0.0024	0.9971
4606	0.244	0.0701	0.0228	0.0024	0.9977	0.232	0.0676	0.0373	0.0027	0.9969
4644	0.215	0.0663	0.0098	0.0010	0.9995	0.263	0.0541	0.0715	0.0051	0.9826
4652	0.236	0.0741	0.0223	0.0023	0.9980	0.196	0.0715	0.0156	0.0011	0.9995
4974	0.214	0.0946	0.0114	0.0012	0.9997	0.243	0.0874	0.0422	0.0030	0.9976
4984	0.194	0.0998	0.0095	0.0010	0.9998	0.270	0.0849	0.0535	0.0038	0.9960
4992	0.180	0.0935	0.0070	0.0007	0.9999	0.264	0.0869	0.0546	0.0039	0.9960
4995	0.182	0.0894	0.0113	0.0011	0.9997	0.210	0.0808	0.0230	0.0016	0.9992
4998	0.207	0.0856	0.0107	0.0011	0.9997	0.175	0.0812	0.0744	0.0053	0.9916
5071	0.209	0.1168	0.0136	0.0015	0.9997	0.197	0.0979	0.0327	0.0023	0.9989
5074	0.168	0.1102	0.0119	0.0013	0.9997	0.286	0.0848	0.0598	0.0043	0.9950
5075	0.183	0.1190	0.0116	0.0013	0.9998	0.284	0.0950	0.0429	0.0031	0.9979
5090	0.251	0.1243	0.0167	0.0018	0.9996	0.355	0.0992	0.0441	0.0031	0.9980
5092	0.235	0.1190	0.0129	0.0014	0.9997	0.336	0.0912	0.0457	0.0033	0.9975
5093	0.174	0.1023	0.0062	0.0007	0.9999	0.252	0.0826	0.0470	0.0033	0.9967
5094	0.182	0.1096	0.0076	0.0008	0.9999	0.196	0.0886	0.0251	0.0018	0.9992
5096	0.219	0.1161	0.0143	0.0015	0.9996	0.278	0.0955	0.0524	0.0037	0.9970
5098	0.191	0.1060	0.0108	0.0012	0.9998	0.280	0.0868	0.0609	0.0043	0.9950
5099	0.247	0.1386	0.0161	0.0017	0.9997	0.260	0.1072	0.0128	0.0009	0.9999
5116	0.226	0.1185	0.0304	0.0033	0.9985	0.320	0.0906	0.0620	0.0044	0.9953
5119	0.200	0.1149	0.0117	0.0013	0.9998	0.295	0.0892	0.0288	0.0020	0.9986